PNL-6593
UC-313

18J

Inert Electrode Program

Immersion Tests of TiB_2-Based Materials for Aluminum Processing Applications

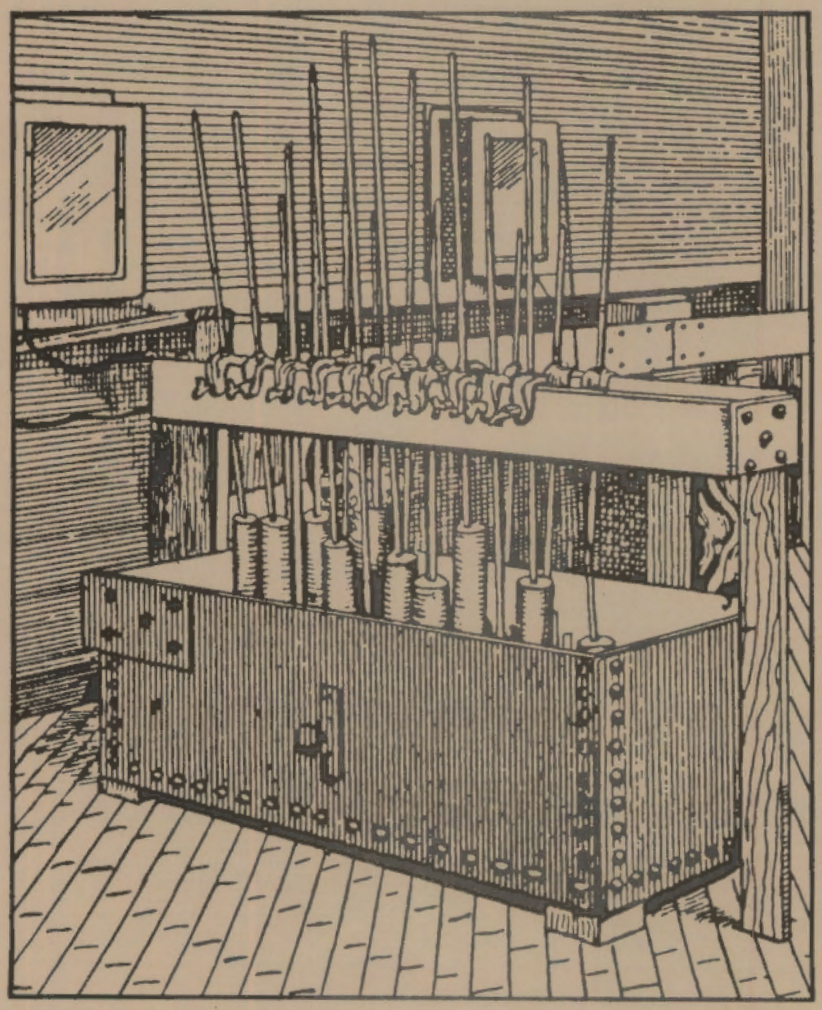

July 1988

Prepared for the U.S. Department of Energy
under Contract DE-AC06-76RLO 1830

Pacific Northwest Laboratory
Operated for the U.S. Department of Energy
by Battelle Memorial Institute

Battelle

PNL-6593

On the cover:

Aluminum reduction pots at the Pittsburgh Reduction Company's (Alcoa's) plant in 1889. Adapted from a photograph, courtesy of Alcoa.

DISCLAIMER

This report was prepared as an account of work sponsored by an agency of the United States Government. Neither the United States Government nor any agency thereof, nor Battelle Memorial Institute, nor any or their employees, makes any warranty, expressed or implied, or assumes any legal liability or responsibility for the accuracy, completeness, or usefulness of any information, apparatus, product, or process disclosed, or represents that its use would not infringe privately owned rights. Reference herein to any specific commercial product, process, or service by trade name, trademark, manufacturer, or otherwise does not necessarily constitute or imply its endorsement, recommendation, or favoring by the United States Government or any agency thereof, or Battelle Memorial Institute. The views and opinions of authors expressed herein do not necessarily state or reflect those of the United States Government or any agency thereof, or Battelle Memorial Institute.

PACIFIC NORTHWEST LABORATORY
operated by
BATTELLE MEMORIAL INSTITUTE
for the
UNITED STATES DEPARTMENT OF ENERGY
under Contract DE-AC06-76RLO 1830

Printed in the United States of America
Available from
National Technical Information Service
United States Department of Commerce
5285 Port Royal Road
Springfield, Virginia 22161

NTIS Price Codes
Microfiche A01

Printed Copy

Pages	Price Codes
001-025	A02
026-050	A03
051-075	A04
076-100	A05
101-125	A06
126-150	A07
151-175	A08
176-200	A09
201-225	A010
226-250	A011
251-275	A012
276-300	A013

3 3679 00056 0153

PNL-6593
UC-313

IMMERSION TESTS OF TiB_2-BASED MATERIALS FOR ALUMINUM PROCESSING APPLICATIONS

C. H. Schilling
G. L. Graff

July 1988

Prepared for
the U.S. Department of Energy
under Contract DE-AC06-76RLO 1830

Pacific Northwest Laboratory
Richland, Washington 99352

SUMMARY

The behavior of four types of TiB_2-based materials exposed to molten Al at 970°C was evaluated for time durations of up to 20 wk. These materials are prime candidates for cathodes in advanced Al smelters and include 1) high-purity polycrystalline titanium diboride (TiB_2), 2) TiB_2-graphite (TiB_2-G) composites, 3) composites of woven ceramic fiber mesh coated with high-purity TiB_2, and 4) composites of 50 vol% TiB_2-50 vol% aluminum nitride (AlN). The evaluations primarily involved optical ceramographic comparisons of samples before and after nonpolarized immersion in molten Al.

The samples of TiB_2-AlN and high-purity TiB_2 exhibited superior resistance to chemical attack by molten Al; no visible microcracking or intergranular penetration by Al was observed. A reaction layer grew to 20 μm in thickness at the surfaces of the TiB_2-AlN after exposure to Al for 20 wk; additional analyses are needed to determine the chemistry of the reaction layer.

The TiB_2-ceramic fiber mesh samples exhibited mixed results; the TiB_2 coatings remained largely intact after 20 wk of exposure to Al, but the SiC-based fibers were attacked within 4 wk of exposure to molten Al. Fiber deterioration may be attributed to chemical reactions between molten Al and reactive constituents of the SiC-based fibers. An evaluation of composites with ceramic fibers that are less susceptible to degradation is recommended.

The TiB_2-G composites exhibited poor resistance to chemical attack by molten Al. The experiments indicate that the surfaces of the composites are attacked by a three-step process: 1) removal of graphite accompanied by penetration of the TiB_2 pores by Al, 2) formation of Al-filled microcracks along TiB_2 grain boundaries, and 3) disruption of the microstructure by extension of large Al-filled cracks. Samples that were exposed for 4 to 20 wk were completely disrupted by Al-filled crack systems and TiB_2 grain boundary penetration by Al. Such catastrophic deterioration does not agree with the satisfactory performance observed with TiB_2-G cathodes during Hall-Heroult cell electrolysis. Additional research is needed to elucidate the chemical reactions causing the difference in performance during polarized

CONTENTS

FIGURES

INTRODUCTION

The Inert Electrode Program is being conducted by Pacific Northwest Laboratory (PNL)[a] for the U.S. Department of Energy, Office of Industrial Programs. The purpose of the program is to develop long-lasting, energy-efficient anodes, cathodes, and ancillary equipment for Hall-Heroult cells used for commercial production of Al. The program is divided into three tasks with the following objectives:

- Inert Anode Development - to improve the energy efficiency of Hall-Heroult cells by development of inert anodes.
- Stable Cathode Development - to develop methods for retrofitting commercial Hall-Heroult cells with titanium diboride (TiB_2)-based cathode materials.
- Sensor Development - to develop sensors to control the bath chemistry of Hall-Heroult cells being operated with stable anodes and cathodes.

Enhanced energy efficiency during the electrolytic production of Al is possible using Al-wetted, TiB_2-based cathodes which reduce voltage drop across the electrolyte by reducing the anode-cathode spacing. Several previous attempts to develop practical cell designs have been unsuccessful because of chemical attack of TiB_2-based cathode materials and poor methods of attaching these materials to the electrolysis cell.[b]

This report summarizes molten Al immersion tests conducted under the Stable Cathode Development task to evaluate the microstructural behavior of TiB_2-based materials. Abbreviated summaries of these experiments are reported by Strachan et al. 1988 (draft)[c] and Schilling (1988). Four types

---

(a) Operated for DOE by Battelle Memorial Institute under Contract DE-AC06-76RLO 1830.

(b) Published research pertaining to Al cathodes for the Al industry is reviewed by Billiehaug and Oye (1980) and Schilling, Hagen, and Hart (1987).

(c) Strachan, D. M. et al. Inert Anode/Cathode Program Fiscal Year 1987 Annual Report. Pacific Northwest Laboratory, Richland, Washington. Draft report to sponsor.

of TiB_2-based materials were evaluated before and after nonpolarized exposure to molten Al at temperatures encountered in Hall-Heroult cells. Three of the materials, TiB_2-graphite (TiB_2-G) composites, TiB_2-aluminum nitride (AlN) composites, and high-purity TiB_2 sintered from halide plasma reduction powders, were chosen because they are prime candidates for Al-wetted cathode applications, based on a literature review (Schilling, Hagen, and Hart 1987) and previous experimental research at PNL (Hart et al. 1987). Ceramic fiber mesh coated with chemical-vapor-infiltrated TiB_2 was also evaluated, based on the expected wear resistance of the high-purity TiB_2 coatings and the possibility of designing advanced cells with complex cathode shapes that are not possible using traditional powder-sintering techniques.

Nonpolarized exposure tests, although not representing actual service conditions for Hall-Heroult cell cathodes, are useful for analyzing possible attack mechanisms that are related to chemical reactions between molten Al and cathode constituents.

In the following sections, the experimental procedure for the immersion tests is described and test results are discussed.

EXPERIMENTAL PROCEDURE

Four types of TiB_2-based materials were examined optically before and after nonpolarized exposure to molten Al at 970°C for time periods of 4, 10, and 20 wk. The four materials are listed below:

1. Woven preforms of SiC-based fibers coated with chemical-vapor-infiltrated TiB_2.(a) Test samples were provided by T. Besmann of Oak Ridge National Laboratory.
2. Single-phase polycrystalline TiB_2 sintered from high-purity powders produced by the Alcoa halide vapor-reduction plasma process (Hoejke 1981; Baumgartner 1984a and 1984b; Baumgartner and Steiger 1984). Test samples were provided by R. Baumgartner of Alcoa Laboratories.
3. Composites of 50 vol% TiB_2-50 vol% AlN. These samples were produced at PNL by hot pressing a mixture of TiB_2 and AlN powder.(b) Uniaxial hot pressing was performed using 5000 psi die pressure at 1850°C under a flowing Ar atmosphere.
4. Composites of TiB_2-G Type B, which were provided by L. Joo of Great Lakes Research Corporation.

Samples from the Type 2, 3, and 4 materials were cut with a diamond saw into 1 cm-by-1 cm pieces. The Type 1 material was cut into samples by the supplier. The samples were then prepared for ceramographic polishing and optical photomicrography.

The Al used for the immersion tests came in the form of pellets measuring approximately 8 mm in diameter.(c) The purity of the as-received Al was evaluated by M. Johnson and H. Hillegass of the Alcoa plant in Wenatchee,

---

(a) The chemical vapor infiltration process is described by Caputo and Lackey (1984), Caputo, Lackey, and Stinton (1985), and Stinton et al. (1986). Samples contained Nicalon SiC-based fibers produced by Nippon Carbon Co., Tokyo, Japan.

(b) The TiB_2 powders were 1 to 5 μm in diameter, the AlN powders were less than 44 μm in size. The powders were supplied by Aremco Corp., Ossining, New York.

(c) J. T. Baker Chemical Co., purified Al shot #0456-1, Phillipsburg, New Jersey.

Washington, using spark emission spectroscopy. Results of this analysis are indicated in Table 1. Major impurities were Fe, Si, Ga, and V, at concentrations of 0.05, 0.029, 0.018, and 0.012 wt%, respectively. Purity analyses were not performed on individual Al samples after high-temperature exposure to the TiB_2-based samples in the immersion tests.

The TiB_2-based samples were cleaned with three, 10-min ultrasonic washes in acetone; the Al pellets were cleaned with a 10-min ultrasonic wash in methanol. The test samples and Al pellets were subsequently oven-dried for 12 h at 40°C under a mechanical pump vacuum. After drying, the test samples were placed in individual alumina (Al_2O_3) crucibles. Approximately 50 g of the cleaned Al pellets were subsequently placed into each crucible.

The loaded crucibles were placed into three separate vacuum furnaces designated for the 4-wk, 10-wk, and 20-wk immersion tests. The furnaces were then evacuated with a mechanical pump and backfilled with 99.99% pure Ar to approximately 1 atm absolute pressure. After repeating the evacuation/backfilling sequence three times for each furnace, Ar was passed through each

TABLE 1. Results of Spark Emission Spectroscopy Analysis for As-Received Al Used in Immersion Tests

Element	Concentration, wt%	Element	Concentration, wt%
Fe	0.050	Pb	0.001
Si	0.029	Sn	0.001
Ga	0.018	B	0.0006
V	0.012	Cd	0.000
Ni	0.003	Co	0.000
Zn	0.003	Li	0.000
Ti	0.003	Sr	0.000
Zr	0.002	Ca	0.000
Bi	0.001	Be	0.000
Cu	0.001	Na	0.000
Mn	0.001	Cr	0.000
Mg	0.001		

furnace at 4 to 5 L/h. The furnaces were then heated to a peak temperature of 970°C at approximately 3°C/min. Two additional immersion tests were performed to evaluate early-stage processes of degradation in the TiB_2-G samples; the aforementioned experimental procedures were used to heat these samples in separate furnaces at a peak temperature of 970°C for 1-h and 8-h durations. All TiB_2-based samples were submerged in Al during the immersion tests.

Twenty-six days after the furnaces were started, a heating element failed in the furnace used for the 20-wk test. The furnace had to be cooled to room temperature and the heating element replaced. The samples, already heated at 970°C for 26 d, were reheated. The crucibles used for the 26-d period were replaced to avoid fracturing the Al_2O_3 crucibles upon reheating. The contents, which had cooled to form Al ingots, were removed intact from the crucibles by gently tapping the side of each crucible with a hammer to crack open the Al_2O_3. The ingots were placed in new crucibles and returned to the furnace. The furnace was purged and reheated by the aforementioned procedures. The samples remained at 970°C for the balance of the 20-wk period.

Each furnace was slowly cooled at approximately 3°C/min after its respective test duration, and the loaded crucibles were sectioned with a diamond saw, metallographically polished, and then photographed with an optical microscope. Oil-based liquids were used during polishing. Samples of TiB_2-G were analyzed by x-ray diffraction (XRD) to examine the cut surfaces before and after the 4 wk of exposure to molten Al. All samples were subsequently stored in a vacuum desiccator to minimize moisture absorption.

RESULTS AND DISCUSSION

This section describes the results of the immersion test experiments. Of the four materials analyzed, the TiB_2-G exhibited the least desirable characteristics. Both the high-purity TiB_2 and the TiB_2-AlN exhibited high resisted to chemical attack. The TiB_2-ceramic fiber mesh exhibited mixed results.

GREAT LAKES TITANIUM DIBORIDE GRAPHITE TYPE B COMPOSITES

Great Lakes TiB_2-G Type B composites exhibited poor resistance to chemical attack by molten Al. The TiB_2-G materials were composed of a porous continuous TiB_2 matrix, which exhibited intergranular penetration by Al after exposure to molten Al. Experimental results indicate that the composites are attacked by a three-step process during nonpolarized exposure to molten Al:

1. Within 1 h of exposure to molten Al at 970°C, Al penetrates the sample surfaces through the TiB_2 pores; Al reacts with graphite to form Al_4C_3 in the TiB_2 pores, resulting in removal of the graphite phase. Although the exact mechanism of graphite removal has not been confirmed, the following processes are expected to play a role: aluminum carbide (Al_4C_3) formation and subsequent dissolution of Al_4C_3 into Al, and Al_4C_3 formation and subsequent movement of Al_4C_3 crystals into the Al.
2. Within B h of exposure, the same pattern of Al penetration continues to deeper levels in the sample, and Al-filled microcracks appear along TiB_2 grain boundaries at the outer edges of the Al penetration zones. The intergranular penetration appears to be time dependent, as the microcracks do not always appear at the deeper layers of the Al penetration zones.
3. The intergranular penetration develops into large, Al-filled crack systems that disrupt the outer edges of the penetration zones within 8 h of exposure. Within 1 wk of exposure, entire samples are disrupted by intergranular penetration and large, Al-filled crack systems. Although the exact mechanisms causing the

microcracking and development of large cracks have not been confirmed, the volumetric expansion associated with the formation of Al_4C_3 from graphite appears to play a role by exerting stresses on the TiB_2 pore walls.

Microstructures of Great Lakes TiB_2-G Type B composites before and after exposure to Al at 970°C for 4, 10, and 20 wk are shown in Figures 1 and 2. In the unexposed condition, the TiB_2 phase appears light-colored and interconnected; the dark-colored phase, distributed throughout the pores of the TiB_2, consists of graphite and open porosity. The unexposed sample contains crack patterns in the TiB_2 which are related to materials processing. The source of the cracks and the impact on test behavior are not known.

After exposures of 4, 10, and 20 wk, all of the TiB_2-G samples were penetrated by large Al-filled cracks; in addition, the samples showed extensive penetration of TiB_2 grain boundaries by Al. Nearly identical features were seen in TiB_2-G Type B samples that were exposed to Al at 970°C for 1 wk, as reported in Hart et al. (1987). Another feature common to the samples exposed for 1, 4, 10, and 20 wk is that dark, faceted crystals appear throughout the Al penetrating the TiB_2-G. To simplify the discussion, these dark, faceted crystals will be referred to as "Phase A" (Figure 1). Phase A is expected to be Al_4C_3 because its formation from elemental Al and C is thermodynamically favored at 970°C; -35.1 kcal is the standard Gibbs free energy for the formation of 1 mol of Al_4C_3 at 970°C (Kubaschewski and Alcock 1979).

In addition, XRD analysis of cut surfaces of the unexposed and 4-wk samples of TiB_2-G suggests consumption of graphite by formation of Al_4C_3 during exposure to molten Al (Figure 3). On the exposed sample, Al_4C_3 was detected along with TiB_2 and Al, but graphite was not detected. In contrast, graphite and TiB_2 were the only phases detected on a sample of the unexposed TiB_2-G. Of course, the XRD experiment does not reveal the physical location of the Al_4C_3; therefore, microchemical analysis is needed to confirm whether Phase A is indeed Al_4C_3.

Additional soak tests were performed in Al at 970°C for 1 h and 8 h to evaluate the time sequence of early-stage degradation processes in TiB_2-G

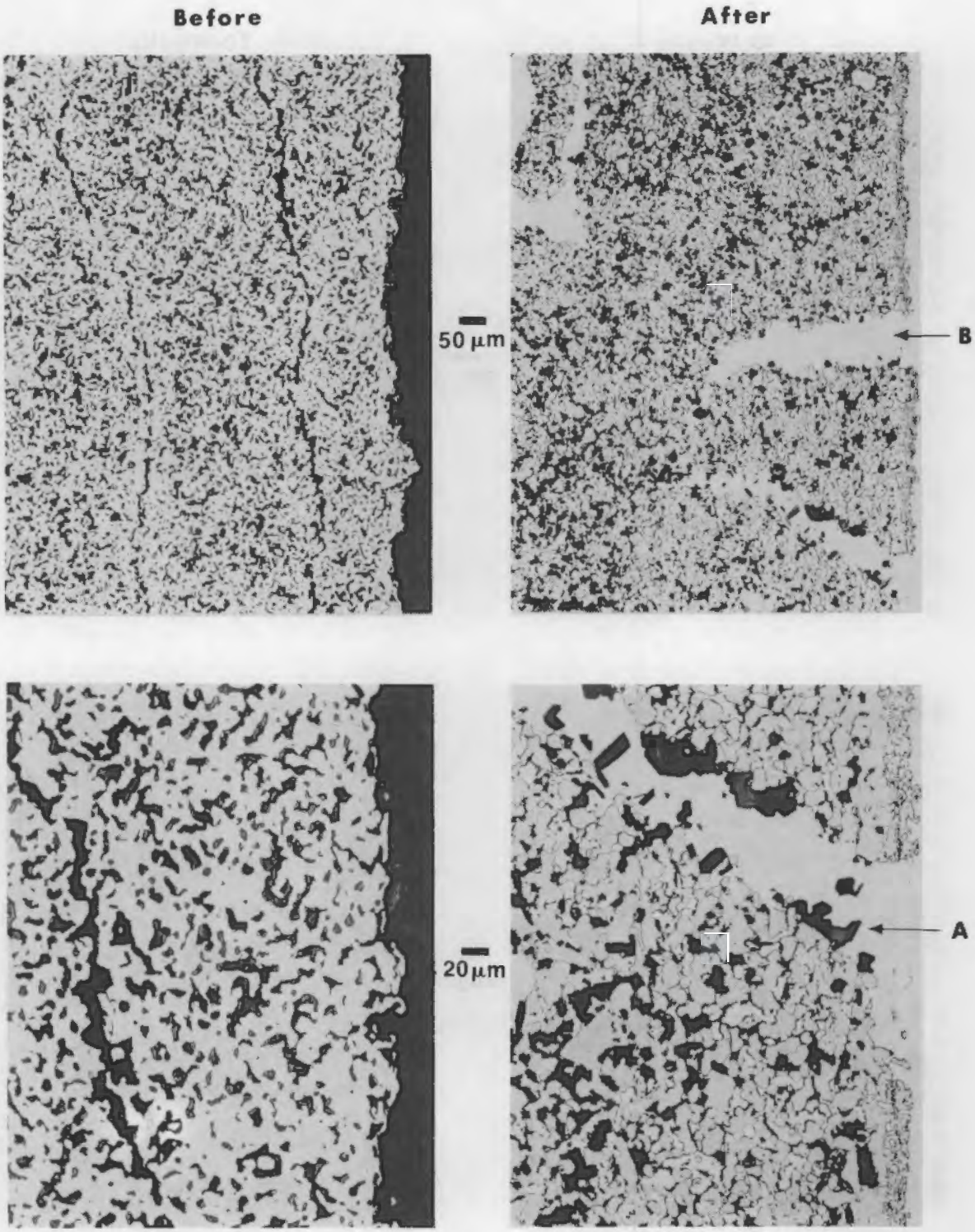

FIGURE 1. Typical Surfaces of Great Lakes TiB_2-G Type B Composite Before and After 4 wk of Exposure to Molten Al at 970°C. Exposure to Al results in formation of faceted crystals (A), possibly Al_4C_3, and large Al-filled crack systems (B).

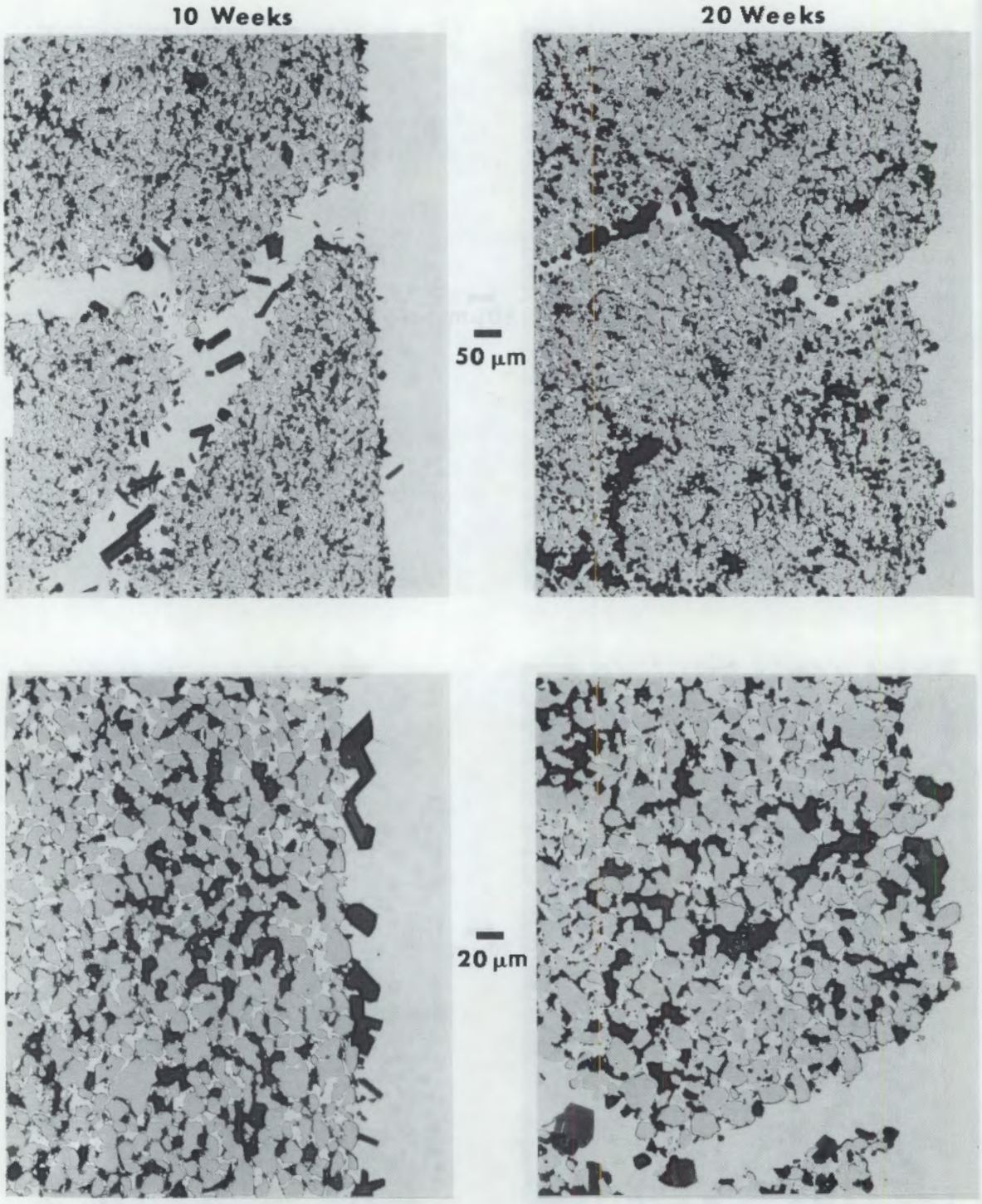

FIGURE 2. Typical Surfaces of Great Lakes TiB_2-G Type B Composite After Exposure to Molten Al for 10 wk and 20 wk at 970°C

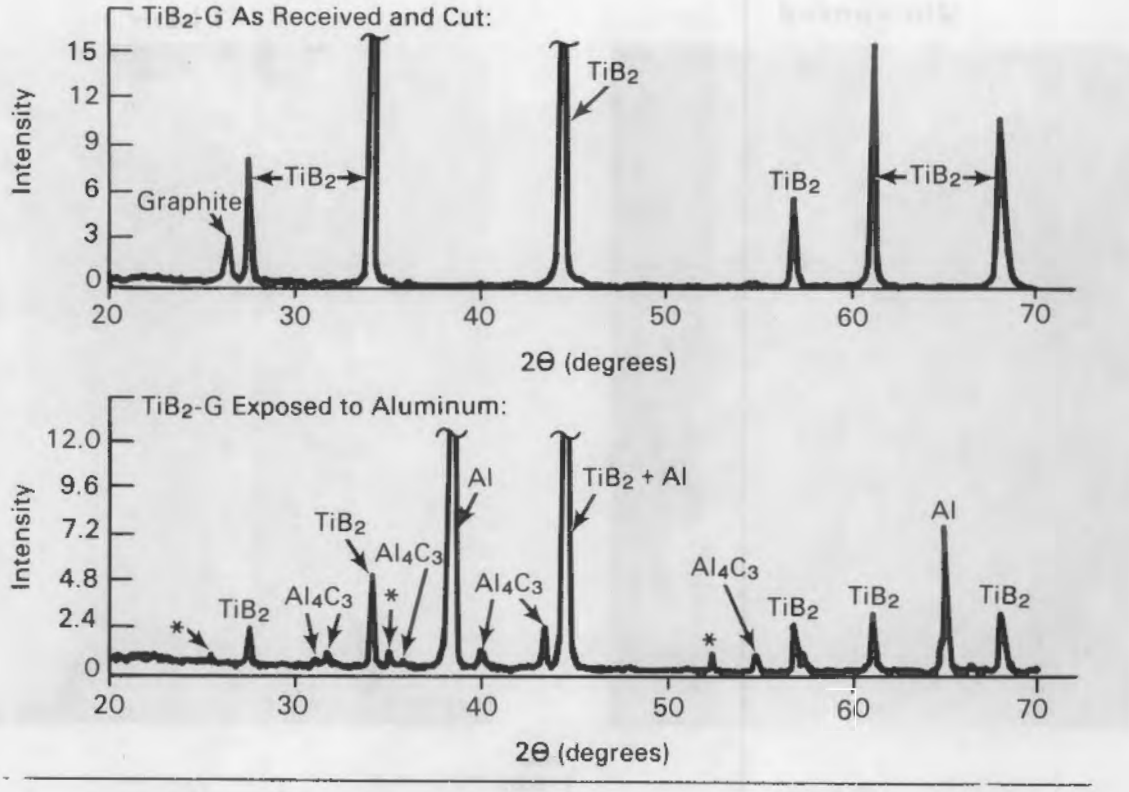

FIGURE 3. X-Ray Diffraction Patterns of TiB_2-G Cut Surfaces Before and After 4-wk Exposure to Molten Al at 970°C. The graphite peak disappears after exposure to Al. * refers to an unknown phase.

Type B materials. Evidence that the surfaces of the composites were attacked during the 1-h and 8-h tests is shown in Figure 4. In a 4-wk exposure, also shown in Figure 4, the entire sample was disrupted by large Al-filled cracks. Within 8 h of exposure, the large, Al-filled cracks appeared at the edges of the sample; in contrast, no cracks were apparent at the surfaces of the 1-h sample though Al penetration had begun to occur. Moreover, the unreacted interior regions of the 1-h and 8-h samples appeared substantially the same as the microstructures of the unexposed samples in Figure 1.

Figures 4 and 5 indicate that, during the 1-h exposure, Al penetrated the upper surface of the composite to a maximum depth of 0.5 to 1.5 mm by replacing graphite contained within the TiB_2 pores. In contrast, the Al penetrated to a maximum depth of 1 to 3 mm during the 8-h exposure (Figures 4 and 6). After 1 h of exposure, the bottom and sides of the TiB_2-G sample exhibited little or no Al penetration. High-magnification micrographs of the

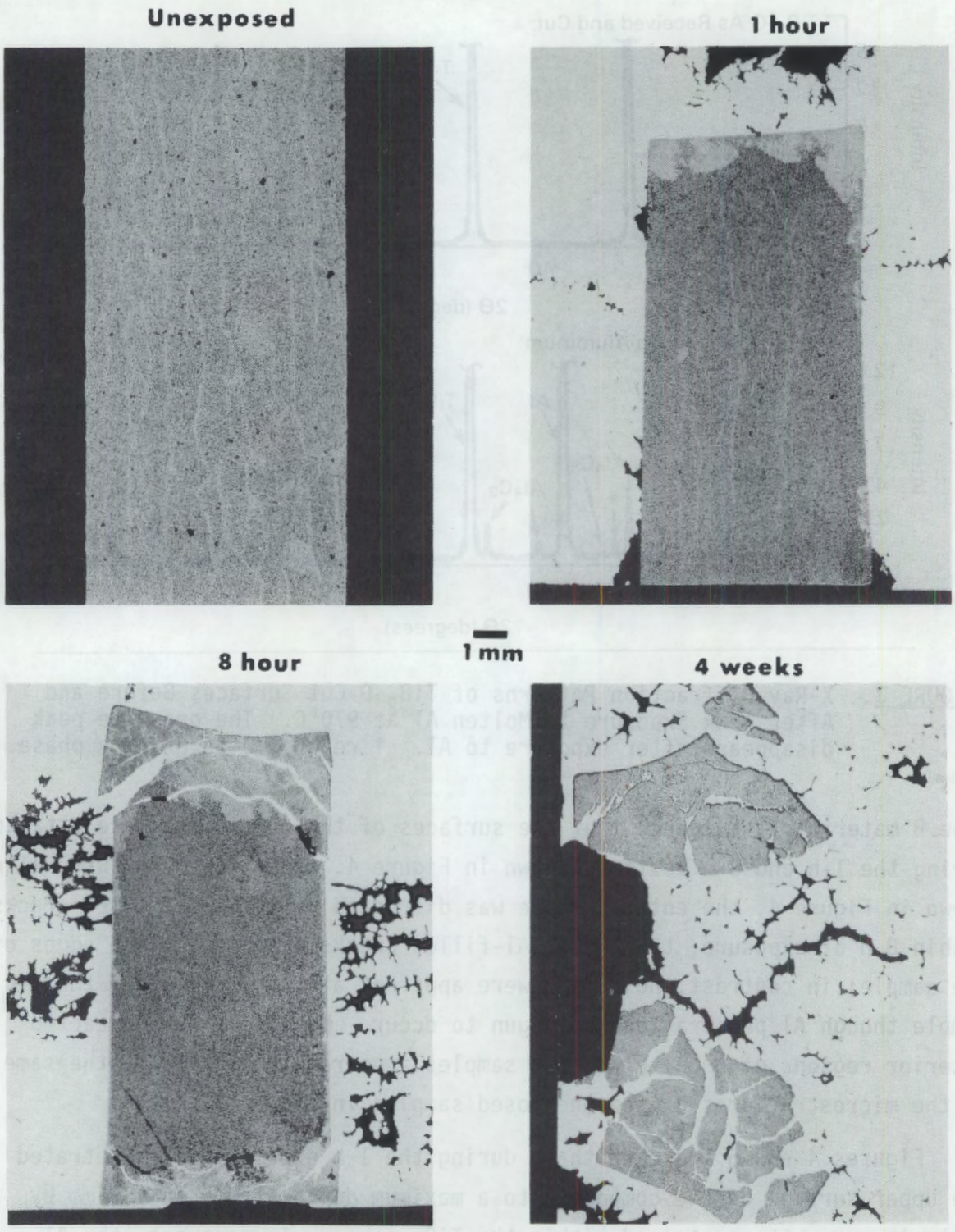

FIGURE 4. Early-Stage Degradation of Great Lakes TiB_2-G Type B Composites Before and After Exposure to Molten Al at 970°C

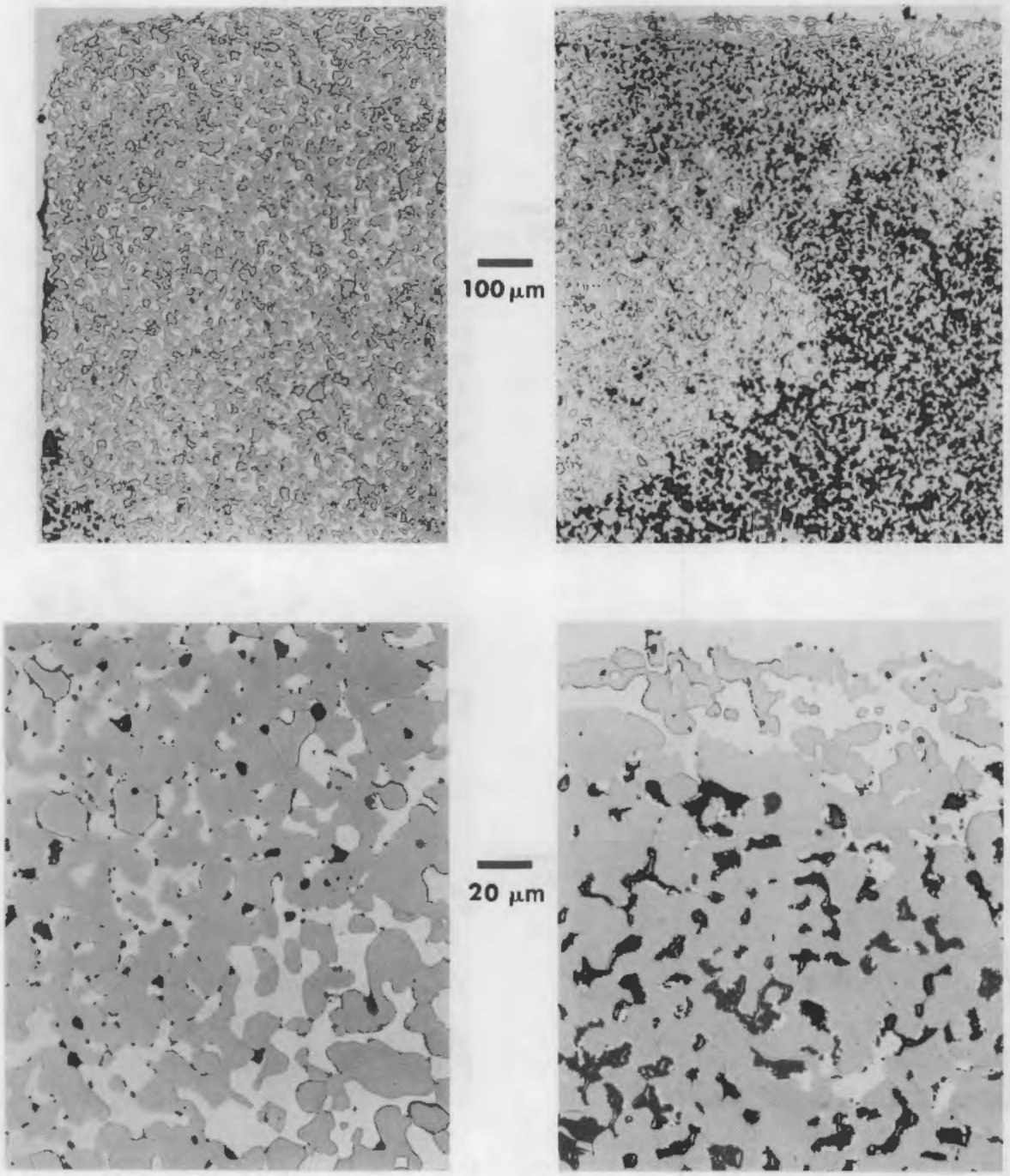

FIGURE 5. Higher Magnifications of 1-h TiB_2-G Test Sample from Figure 4. The upper left corner of the composite is shown on the left. A typical interface between the Al penetration zone and the unreacted interior of the composite is shown on the right.

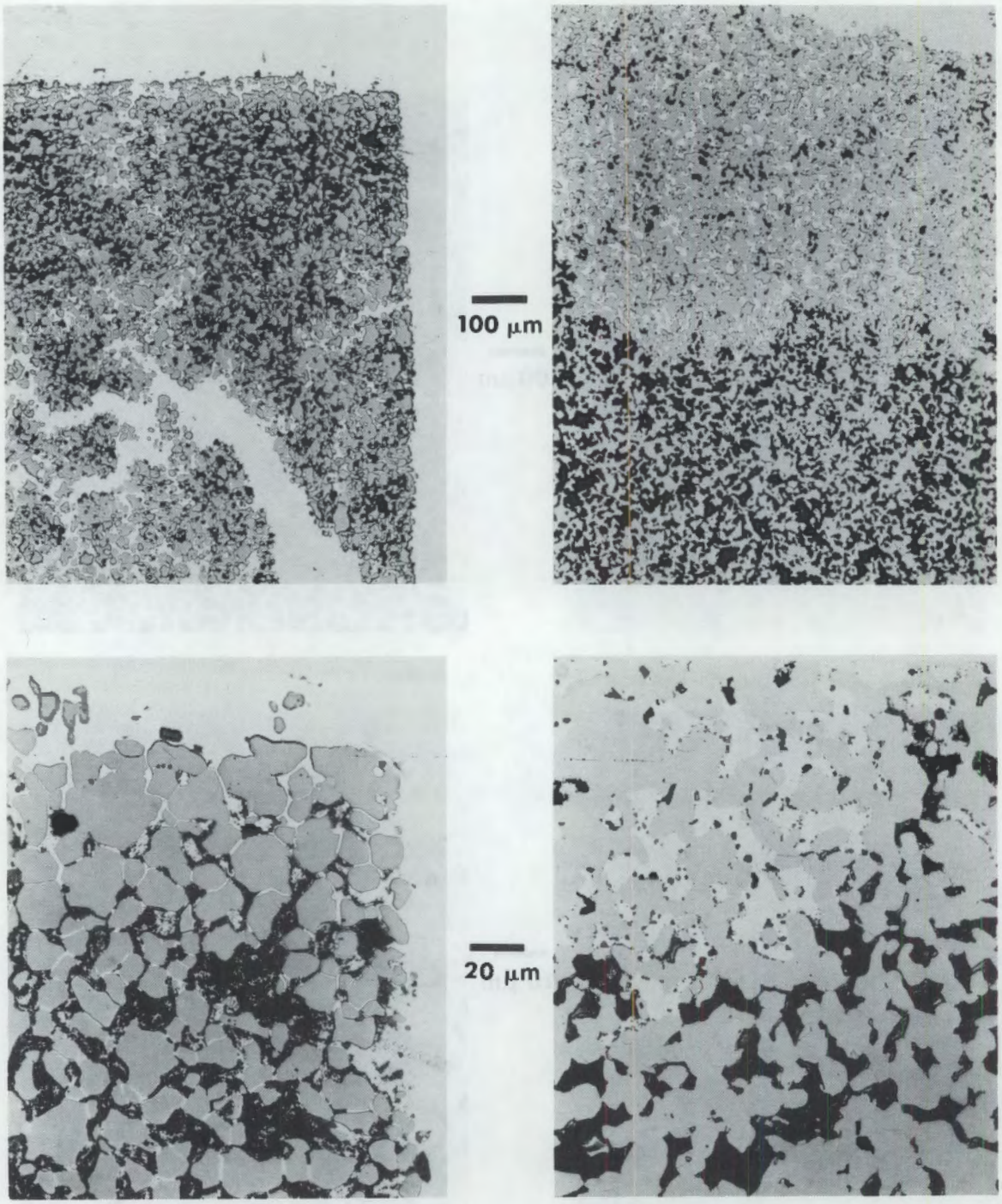

FIGURE 6. Al Penetration Zones in Great Lakes TiB_2-G Type B Composite After Exposure to Molten Al for 8 h at 970°C.[2] Micrographs are higher magnifications of the 8-h sample shown in Figure 4: The upper right corner of the composite is shown at left; typical features at an interface between the Al penetration zone and the unreacted interior of the composite are shown at right.

upper left corner of the 1-h sample did show some Al filling the pores and displacing the graphite (Figure 5). In addition, the Al penetration zones in the 1-h sample exhibited dark phases, which may be graphite and/or Al_4C_3, within the pores of the TiB_2; this dark phase also appeared in the TiB_2 pores of the 8-h sample (Figure 6). As indicated in Figure 5, facets appeared on several of these dark phases; based on comparison with Figure 1, it is possible that these faceted crystals are also Phase A.

Intergranular penetration appears to be a time-dependent process. After 1 h of exposure, microcracks were not visible along TiB_2 grain boundaries in the Al penetration zones (Figure 5). After 8 h of exposure, the Al penetration zones exhibited Al-filled microcracks along TiB_2 grain boundaries, spalling of TiB_2 grains, and development of large, Al-filled cracks extending the width of the specimen (Figures 4 and 6). Further evidence for time-dependent microcrack formation is that intergranular penetration was not uniformly distributed throughout the Al penetration zones in the 8-h sample (Figures 6 and 7). As indicated in Figure 6, intergranular penetration was predominantly observed at the surfaces of the 8-h sample, whereas the microcracks were less frequent near the interfaces between the unreacted interior of the composite and the 1- to 3-mm Al penetration zones at the top and bottom of the composite. Intergranular penetration was also observed predominantly throughout the narrow zones of Al penetration at the sides of the 8-h sample (Figure 7). As indicated in Figure 7, the majority of TiB_2 beneath the penetration zone was not visibly microcracked, although a few microcracks appeared directly beneath the interface between the penetration zone and the unreacted interior of the composite.

Another notable feature of the 8-h sample is that the dark phases were not uniformly distributed in the Al penetration zones. The dark phases were segregated in a large volume fraction of the TiB_2 pore spaces at the four corners of the 8-h sample (Figures 4 and 6). In contrast, the dark phases occupied a smaller amount of the TiB_2 pore spaces near the interfaces between the unreacted interior of the sample and the 1- to 3-mm penetration zones at the top and bottom of the sample (Figure 6). Based on the relatively small quantities of the dark phases observed in the pores of the 1-h sample, redistribution of the dark phase possibly has occurred during the 8-h test.

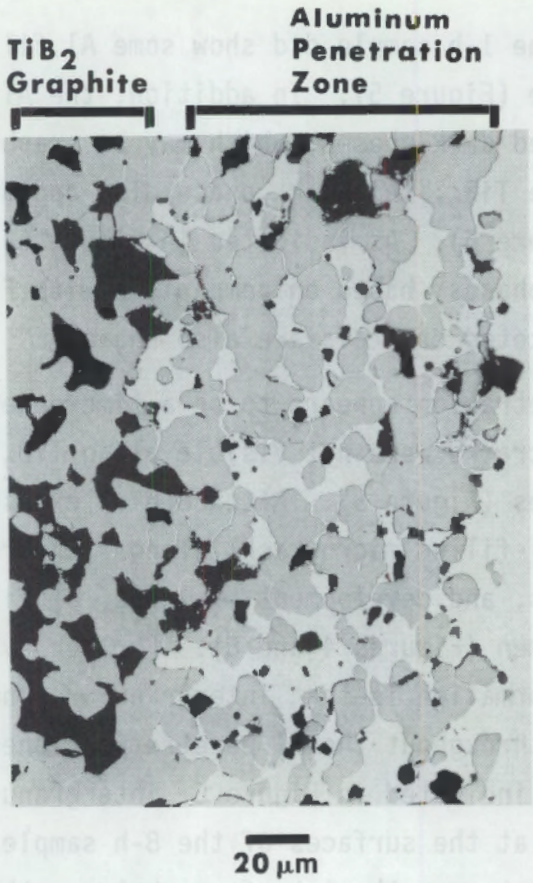

FIGURE 7. Al Penetration Zone at the Surface of Great Lakes TiB_2-G Type B Composite After Exposure to Molten Al for 8 h at 970°C. Micrograph is taken at the right side of the composite shown in Figure 4.

Additional soak tests, with time durations between 1 and 8 h, are needed to elucidate the time sequence of Al penetration, TiB_2 microcracking, and possible redistribution of the dark phase.

Based on all of the above observations, the surfaces of the composites apparently are attacked by a three-step process: 1) removal of graphite accompanied by penetration of the TiB_2 pores by Al, 2) formation of Al-filled microcracks along TiB_2 grain boundaries, and 3) disruption of the microstructure by extension of large, Al-filled cracks. It is plausible that microcracks may develop from stresses caused at least partially by the formation of Al_4C_3 crystals within the TiB_2 pores. Expansion stresses within TiB_2 pores are possible since 1 cm^3 of graphite is expected to form 3.8 cm^3 of

Al_4C_3, based on molar volume calculations (see Appendix). Additional experiments are needed to confirm the mechanism of attack in these composites.

To date, TiB_2-G Type B composites are reported to exhibit satisfactory wear resistance during Hall-Heroult cell cathode tests [Tucker et al. 1986; Tabereaux 1987; Hart et al. 1987; Schilling 1988; Strachan et al. 1988 (draft)[a]]. Additional research is needed to confirm differences in wear mechanisms under conditions of Hall-Heroult cell electrolysis and nonpolarized exposure to molten Al. It is hypothesized that possible differences in behavior may be attributed to differences in the rate at which Al_4C_3 is removed from the TiB_2 pores. Anoxic conditions during the immersion tests are not expected to result in a mechanism for rapid, steady removal of Al_4C_3 from the TiB_2 pores;[b] therefore, it may be suggested that stresses are exerted on the TiB_2 pore walls as a result of Al_4C_3 formation. It is hypothesized that this process may fracture the brittle TiB_2 matrix, subsequently exposing Al to deeper regions of the composite and allowing the attack process to proceed inward from the exterior surfaces. Supporting this hypothesis, molar volume calculations (see Appendix) suggest that if all of the C present formed Al_4C_3, the saturation solubility of dissolved Al_4C_3 in Al would be exceeded by several times during the immersion tests. As a result, dissolution rates would approach zero as the saturation solubility was reached, and Al_4C_3 crystals would be expected to accumulate and remain inside the TiB_2 pores. This proposed degradation process is shown in a schematic illustration in Figure 8.

It is also hypothesized that this form of attack may never occur in a TiB_2-G cathode, because the literature suggests that Hall-Heroult cell conditions favor the rapid removal of Al_4C_3 from Al- graphite interfaces and into the Al. It is possible that this process prevents disruption of the TiB_2 matrix during electrolysis, because of the rapid removal of Al_4C_3 from the

---

(a) Strachan, D. M. et al. Inert Anode/Cathode Program Fiscal Year 1987 Annual Report. Pacific Northwest Laboratory, Richland, Washington. Draft report to sponsor.

(b) Several authors report that oxidizing atmospheres enhance transport of Al_4C_3 from molten Al into the atmosphere: Hollingshead and Brown 1981; Takemoto et al. 1963; Dorward 1973a and 1973b; Grjotheim, Naeumann, and Oye 1977.

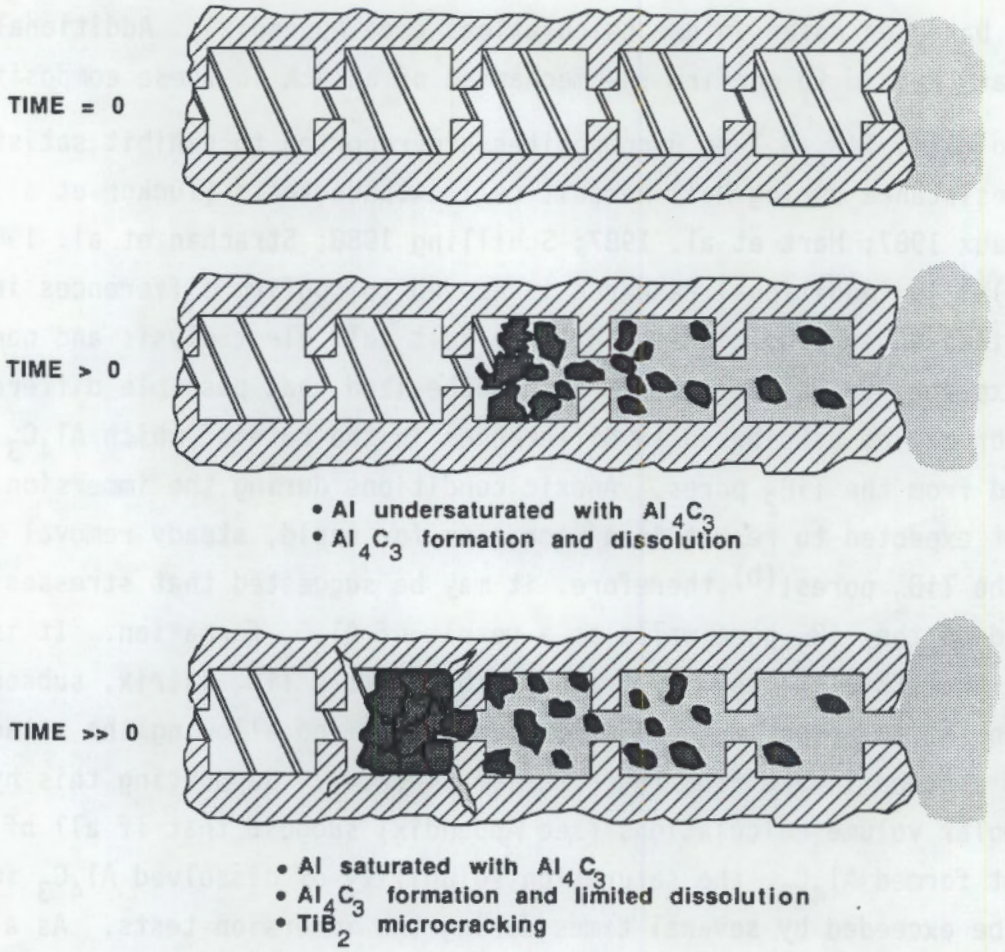

FIGURE 8. Proposed Sequence of TiB_2-G Degradation During Immersion Tests. The TiB_2 pores are schematically represented by a series of square cavities attached by narrow channels. Al_4C_3 accumulates within Al-filled TiB_2 pores; volumetric expansion of the Al_4C_3 relative to graphite may fracture the TiB_2 matrix.

Al-filled TiB_2 pores. In support of this argument, several authors report that Al in Hall cells typically contains Al_4C_3 at concentrations of 10 to 25 ppm, which are well below the saturation solubility of approximately

360 ppm at 960°C. As a result, Al_4C_3 formed at Al-graphite interfaces is expected to dissolve into the metal pad during electrolysis. The Al_4C_3 subsequently diffuses through the Al and cryolite (Na_3AlF_6) bath and is removed from the cell by reacting with CO_2 or O_2 at the anode (Hollingshead and Brown 1981; Takemoto et al. 1963; Dorward 1973a and 1973b; Grjotheim, Naeumann, and Oye 1977). Transport of Al_4C_3 may be by a similar mechanism during electrolysis with cermet anodes. In addition, the existence of a Na-rich layer observed beneath surfaces of TiB_2-G cathodes may affect the rate of Al_4C_3 formation and subsequent dissolution into the Al pad [Schilling 1988; Strachan et al. 1988 (draft)(a)].

ALCOA HIGH-PURITY TiB_2

As seen in Figures 9 and 10, the Alcoa high-purity TiB_2 exhibited resistance to attack after being soaked in Al for up to 20 wk at 970°C. There was no visible microcracking, intergranular penetration by Al, or spalling of TiB_2 grains. The 4-wk samples and the 10-wk samples looked substantially the same as the unexposed sample, with no evidence of attack. In Figure 9, the dark layer at the Al-TiB_2 interface is a photographic artifact caused by a slight curvature of the polished sample surface; by adjusting the focus of the microscope to compensate for this curvature, a sharp Al-TiB_2 interface can be distinguished that is void of features that would suggest a reaction phase. In Figure 10, a dark, faceted phase appears in the Al at the surface of the 20-wk sample. The composition of this phase has not been identified.

The results shown in Figures 9 and 10 are in agreement with Baumgartner's (1984a) observations of insignificant Al penetration into high-purity TiB_2 after soaking in Al at 1200°C for 1 h. However, Baumgartner (1984a) reports that, over a period of months, substantial diffusion of Al may be observed along TiB_2 grain boundaries in these high-purity materials. Baumgartner observed intergranular segregation of Al, Fe, P, and Si to a depth of 400 μm from the surface of a sample that was exposed in a commercial

---

(a) Strachan, D. M. et al. Inert Anode/Cathode Program Fiscal Year 1987 Annual Report. Pacific Northwest Laboratory, Richland, Washington. Draft report to sponsor.

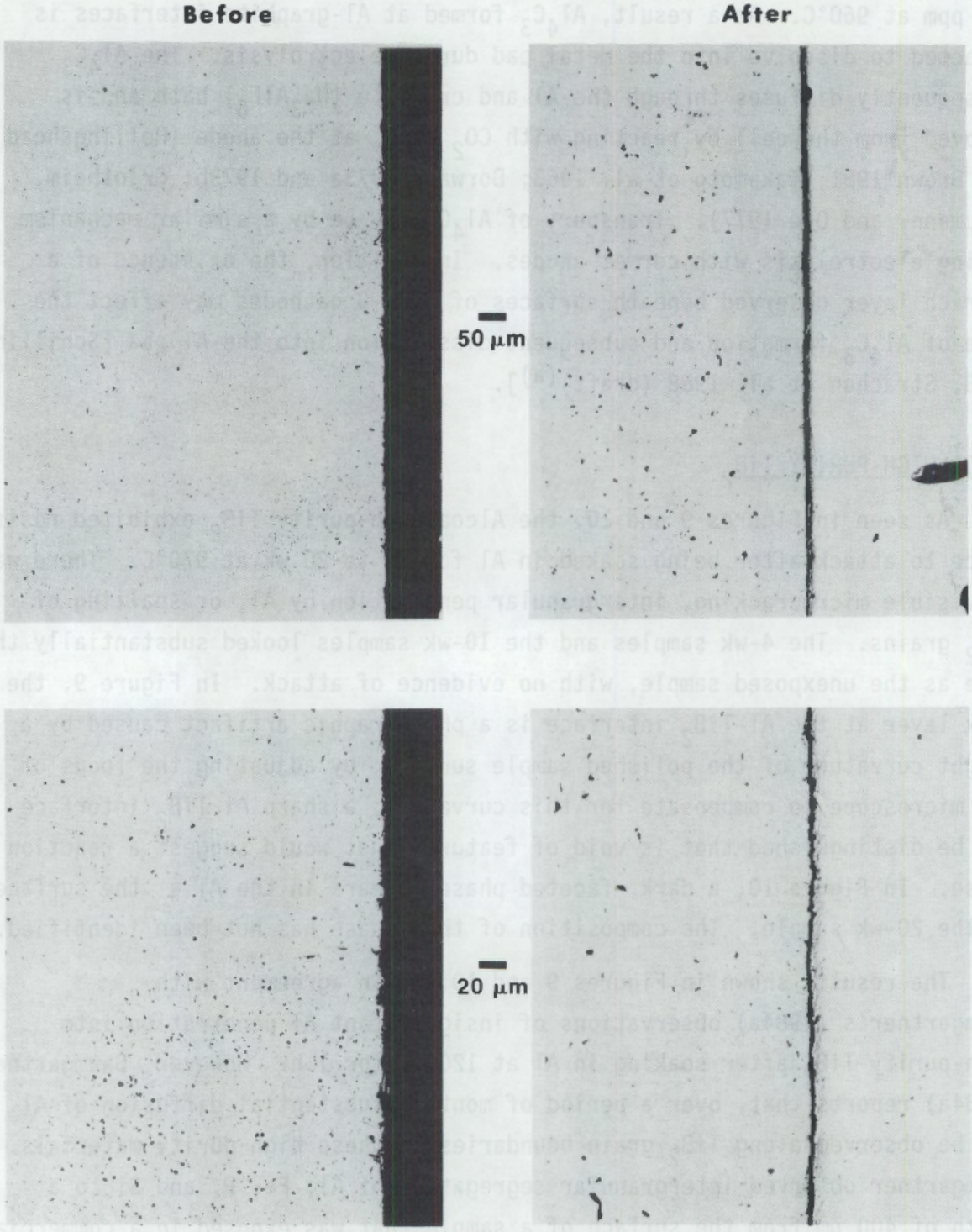

FIGURE 9. Typical Surfaces of Alcoa High-Purity TiB_2 Before and After Exposure to Molten Al at 970°C for 4 wk

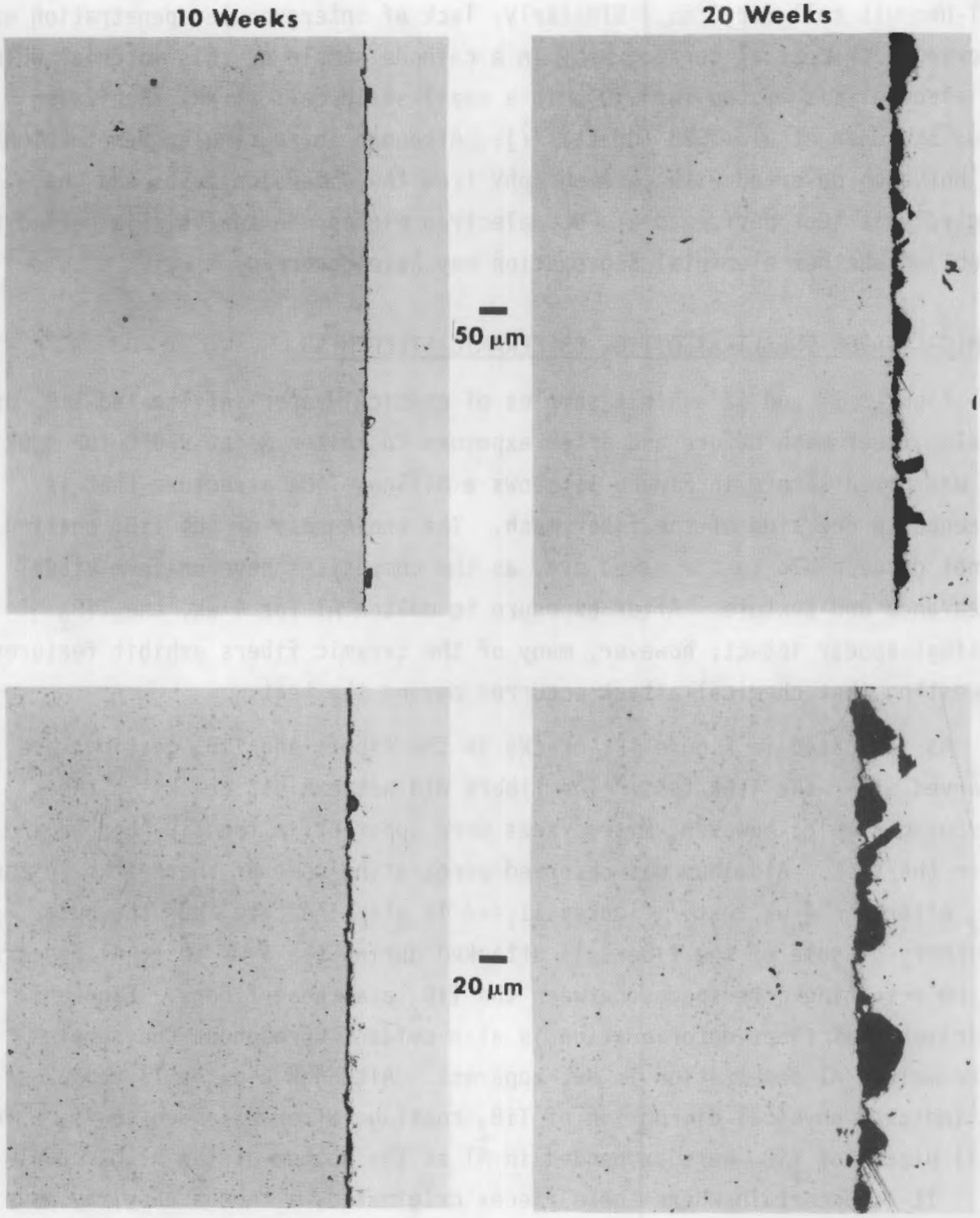

FIGURE 10. Typical Surfaces of Alcoa High-Purity TiB_2 After Exposure to Molten Al at 970°C for 10 wk and 20 wk

Hall-Heroult cell for 6 mo. Similarly, lack of intergranular penetration was observed with optical ceramography in a cathode sample of this material which was electrolysis tested for 140 h in a small-scale cell at PNL [Schilling 1988; Strachan et al. 1988 (draft)(a)]. Although intergranular penetration has not been observed with ceramography from the immersion tests and the electrolysis test performed at PNL, electron microprobe analysis is needed to establish whether elemental segregation may have occurred.

CHEMICAL-VAPOR-INFILTRATED TiB_2 ON CERAMIC FIBER MESH

Figures 11 and 12 exhibit samples of chemical-vapor-infiltrated TiB_2 on Nicalon fiber mesh before and after exposure to molten Al at 970°C for 4 wk. The unexposed sample in Figure 11 shows a billowy TiB_2 structure that is attached to one side of the fiber mesh. The unevenness of the TiB_2 coating is not discernible to the naked eye, as the composites have uniform visual appearance and texture. After exposure to molten Al for 4 wk, the TiB_2 coatings appear intact; however, many of the ceramic fibers exhibit features suggesting that chemical attack occurred during the test.

As indicated in Figure 12, cracks in the fibers and TiB_2 coatings are observed after the 4-wk test. The fibers did not exhibit cracks in the unexposed sample; however, microcracks were apparent in the TiB_2 before and after the test. Aluminum was observed penetrating some of the cracks in the TiB_2 after the 4-wk test. Figures 11 and 12 also indicate that the outer periphery of some of the fibers is attacked during the 4-wk test; Al appears in the resulting pore spaces between the TiB_2 and these fibers. Figure 12 indicates that fiber deterioration is also evident throughout the sample where molten Al penetration is not apparent. Although Figures 11 and 12 do not indicate physical disruption of TiB_2 coatings after exposure to Al, a few small pieces of TiB_2 were suspended in Al at the bottom of the Al_2O_3 crucible. It is uncertain where these pieces originated, although they may have been loose fragments existing in the as-received samples.

(a) Strachan, D. M. et al. Inert Anode/Cathode Program Fiscal Year 1987 Annual Report. Pacific Northwest Laboratory, Richland, Washington. Draft report to sponsor.

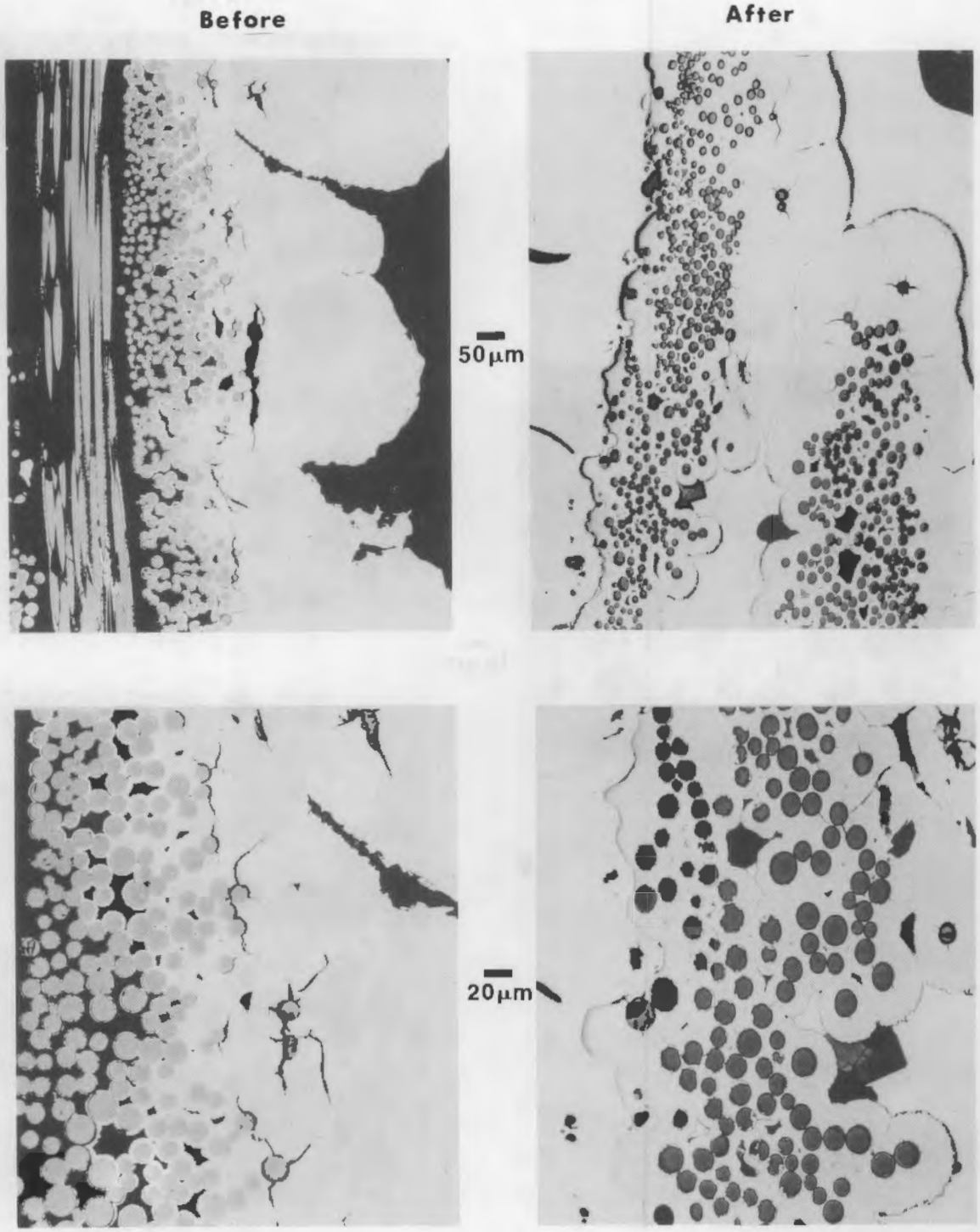

FIGURE 11. Microstructures of Chemical-Vapor-Infiltrated TiB_2 on Nicalon Fiber Mesh Before and After Exposure to Molten Al at 970°C for 4 wk

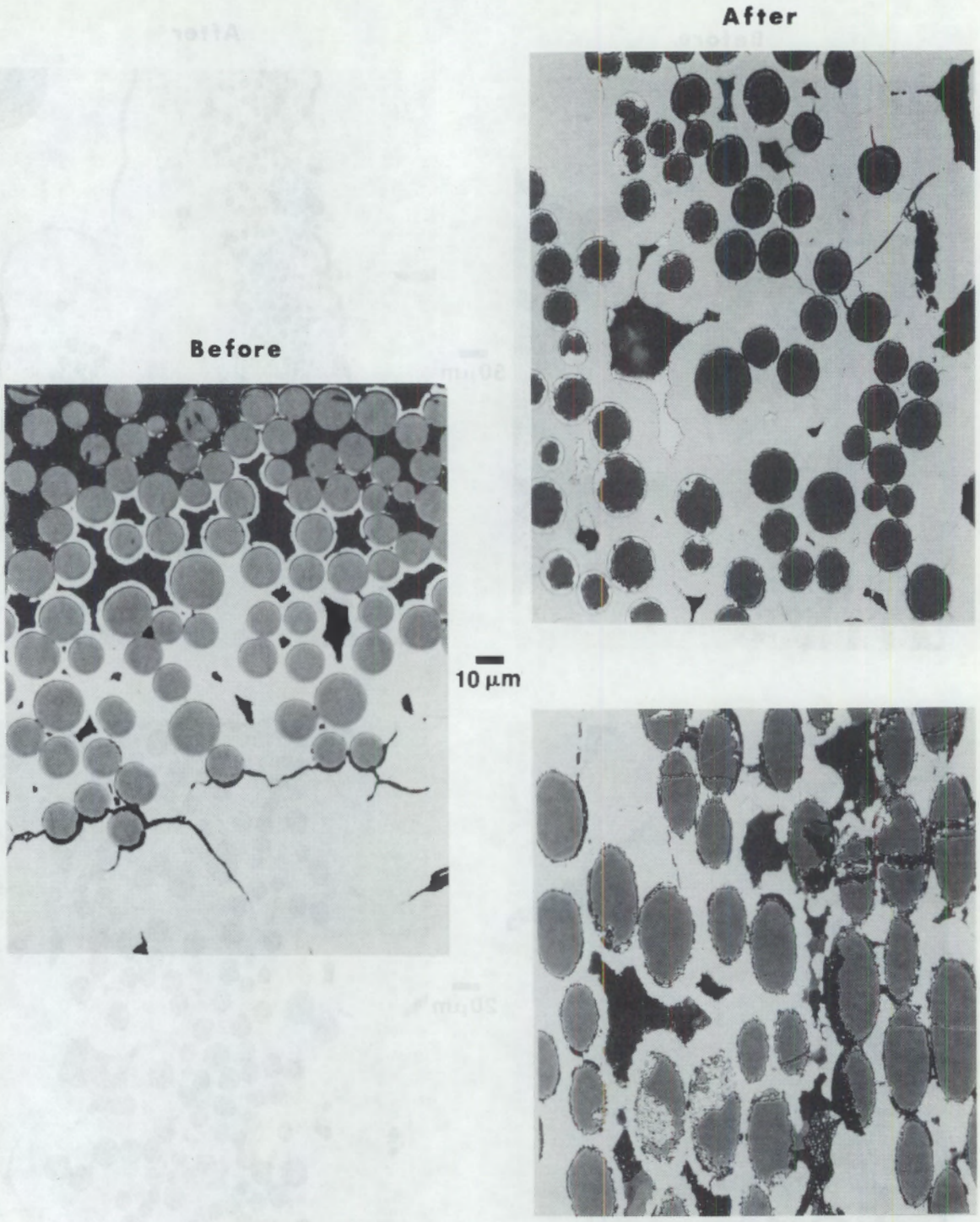

FIGURE 12. Microstructures of Chemical-Vapor-Infiltrated TiB_2 on Nicalon Fiber Mesh Before and After Exposure to Molten Al at 970°C for 4 wk Shown at Higher Magnification

Penetration by Al and deterioration of the ceramic fibers are more pronounced in the samples that were exposed to molten Al for 10 wk and 20 wk. As indicated in Figures 13 and 14, the TiB_2 coatings appear largely intact after the 10-wk and 20-wk tests, although the TiB_2 has deteriorated in regions near the fibers. After exposure to molten Al for 20 wk, some of the fibers have disappeared altogether.

The deterioration seen in the Nicalon fibers may be a result of chemical reactions between Al and reactive constituents of the fibers, such as C and SiO_2. The as-received Nicalon fibers consist of ultrafine beta SiC crystals (10 to 25 Å dia.) which are homogeneously distributed in an amorphous phase containing C and SiO_2 (Andersson and Warren 1984; Chaim, Heuer, and Chen 1988; Schoenlein et al. 1988; Jones et al. 1988). Based on reaction thermodynamic arguments, it is plausible that the C and SiO_2 originally present in the fibers reacted with Al to produce more stable phases such as Al_4C_3 and Al_2O_3 (Brondyke 1953; Standage and Gani 1967; Kubaschewski and Alcock 1979).

Thermal degradation of the Nicalon fibers may also play a role in the attack of the fibers during exposure to molten Al. Luthra (19B6), Simon and Bunsell (1984), Clark et al. (1985), Mah et al. (1984), and Johnson et al. (1988) report that, without molten Al present, Nicalon SiC fibers thermally degrade above 1000°C to form phases such as SiO_2 and CO as a result of excess Si, C, O, and N in the as-received fibers. Based on reaction thermodynamic arguments, thermal degradation phases such as SiO_2 and CO may have reacted with molten Al to form some of the reaction phases appearing in Figures 11 through 14. Additional research is needed to confirm the chemical reactions responsible for fiber degradation. Based on the result that the TiB_2 coatings remain largely intact after the 20-wk test, evaluation of similar composites made of ceramic fibers that are less susceptible to deterioration by Al is recommended. Possible fiber candidates which are currently being developed by various ceramic industries include AlN, BN, Al_2O_3, and high-purity SiC (Romine 1987).

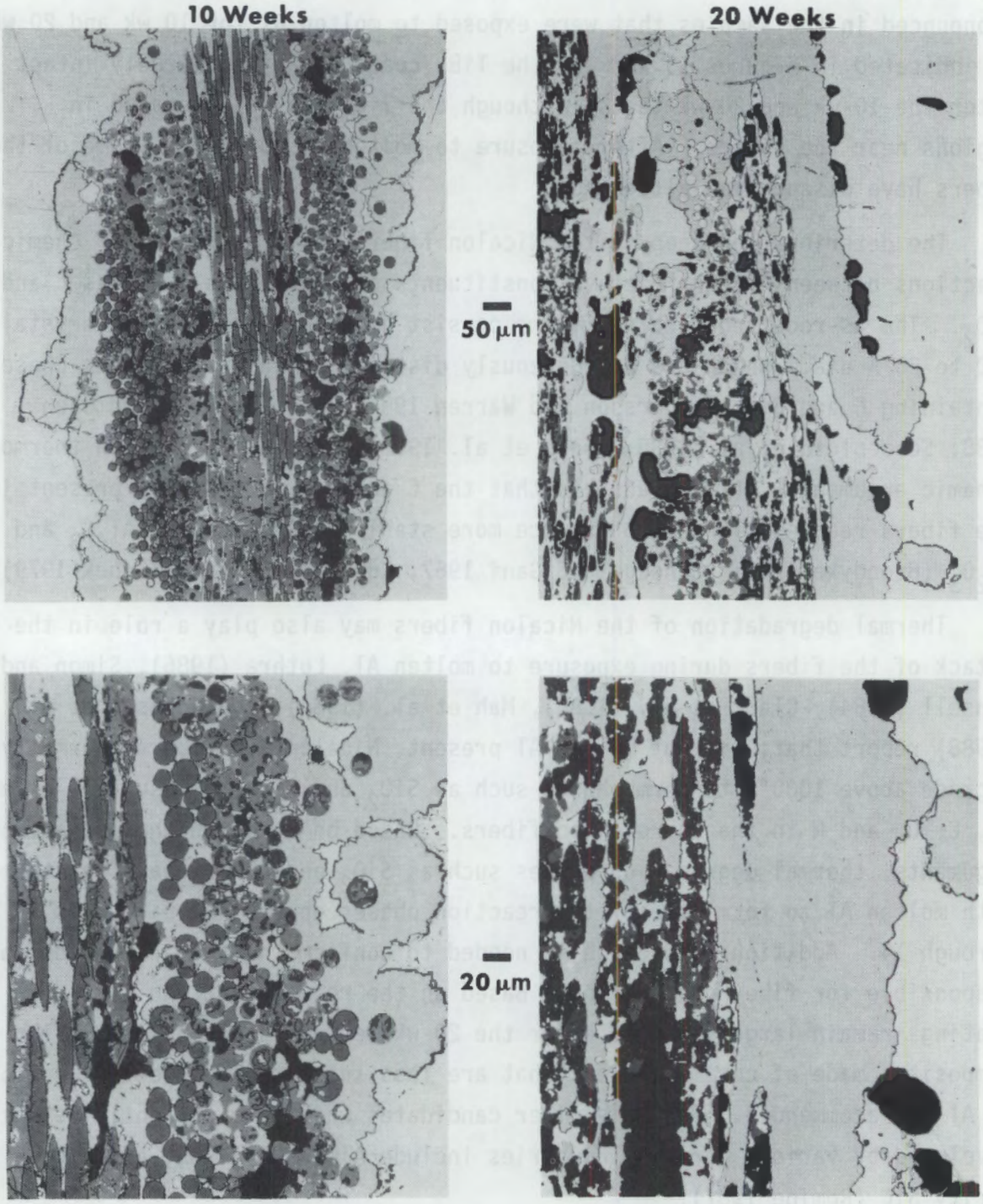

FIGURE 13. Microstructures of Chemical-Vapor-Infiltrated TiB_2 on Nicalon Fiber Mesh After Exposure to Molten Al at 970°C for 10 wk and 20 wk

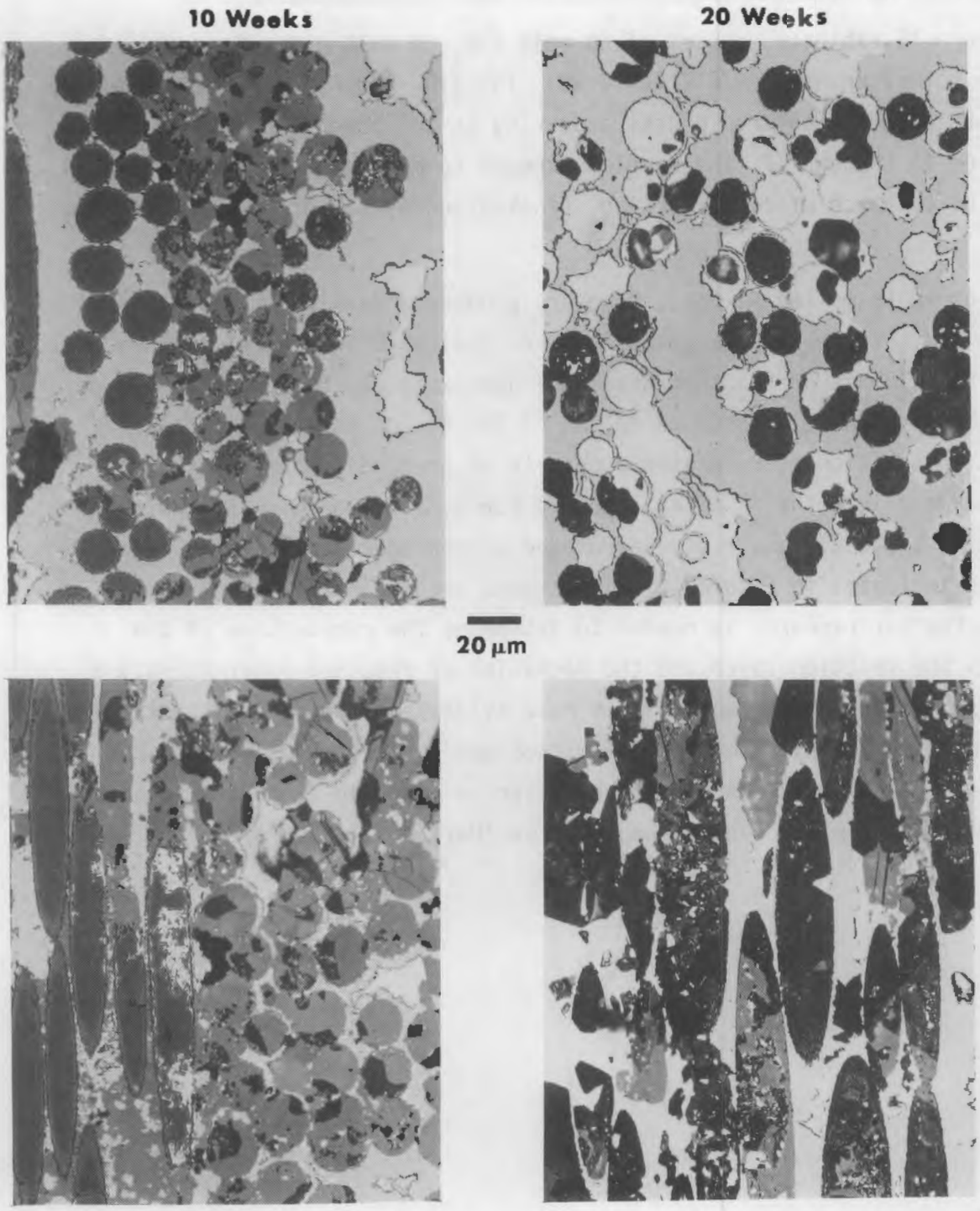

FIGURE 14. Microstructures of Chemical-Vapor-Infiltrated TiB_2 on Nicalon Fiber Mesh After Exposure to Molten Al at 970°C for 10 wk and 20 wk Shown at Higher Magnification

COMPOSITES OF 50 vol% TITANIUM DIBORIDE-50 vol% ALUMINUM NITRIDE

Figure 15 exhibits samples of 50 vol% TiB_2-50 vol% AlN before and after exposure to molten Al at 970°C for 4 wk. The TiB_2 and AlN are, respectively, the light- and dark-colored phases appearing in the composite. As indicated in Figures 15 through 17, the samples exposed to molten Al for 4, 10, and 20 wk show no evidence of microcracking, penetration by Al, or spalling of TiB_2 or AlN.

Exposure to molten Al does, however, produce a dark-colored reaction layer at the surfaces of the composite. As indicated in Figures 15 through 17, the reaction layer has thicknesses of approximately 5, 10, and 20 μm on the samples that were exposed to molten Al for 4, 10, and 20 wk, respectively. In addition, TiB_2 grains appear to be protruding through the reaction layer and into the Al after exposure for 4, 10, and 20 weeks, which suggests that the AlN phase may be removed at the reaction layer/Al interface. As indicated in Figure 16, microcracks appear in these protruding grains. Further research is needed to determine the composition of the phases in the reaction layer and the mechanism of reaction layer formation. It is possible that these samples may have evidence of chemical attack which is beyond detection with the optical microscope. Electron microscopy has been used to show grain boundary penetration in TiB_2-AlN samples exposed to molten Al under similar conditions for 1 wk (Hart et al. 1987).

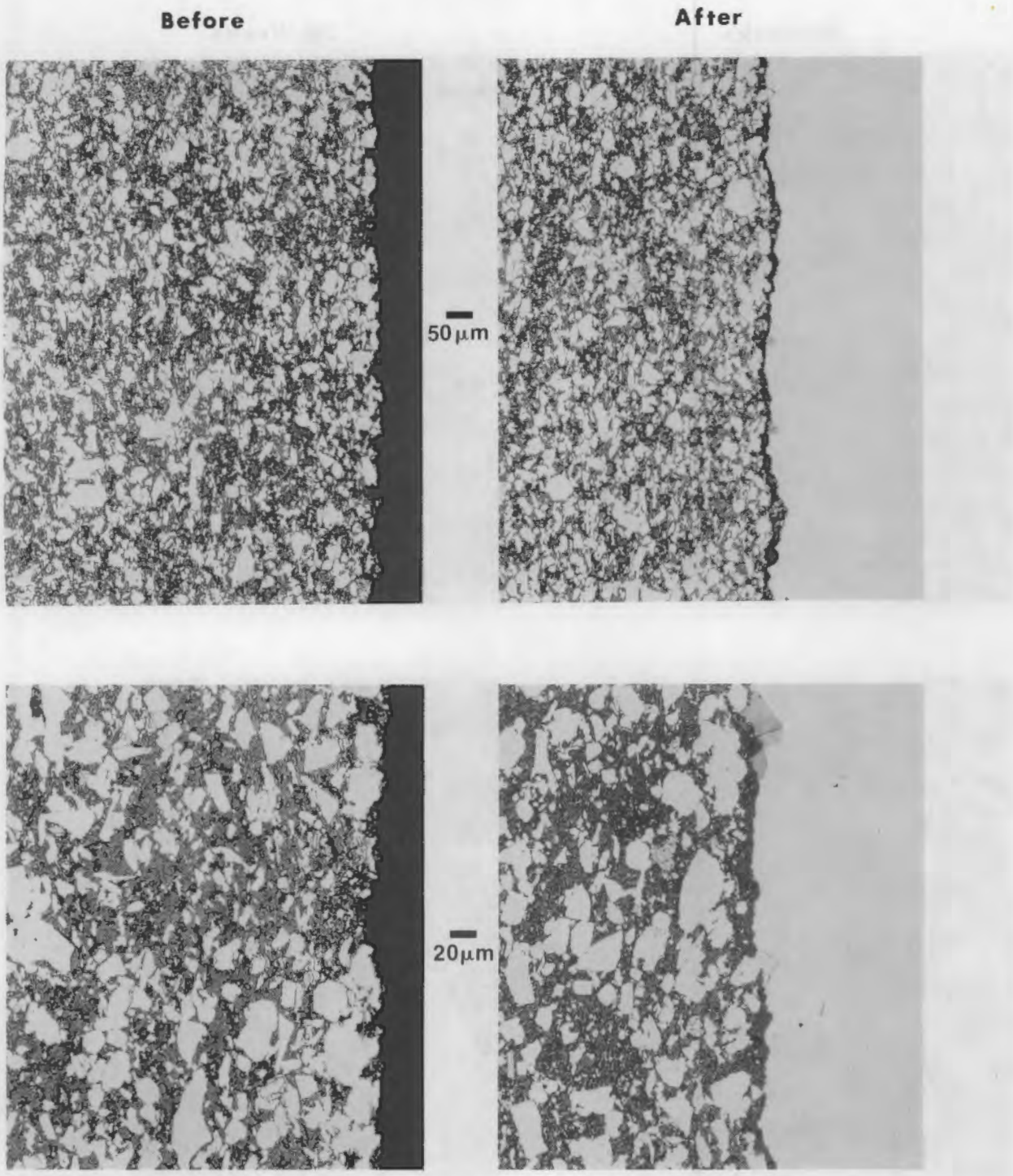

FIGURE 15. Typical Surfaces of 50 vol% TiB_2-50 vol% AlN Before and After Exposure to Molten Al for 4 wk

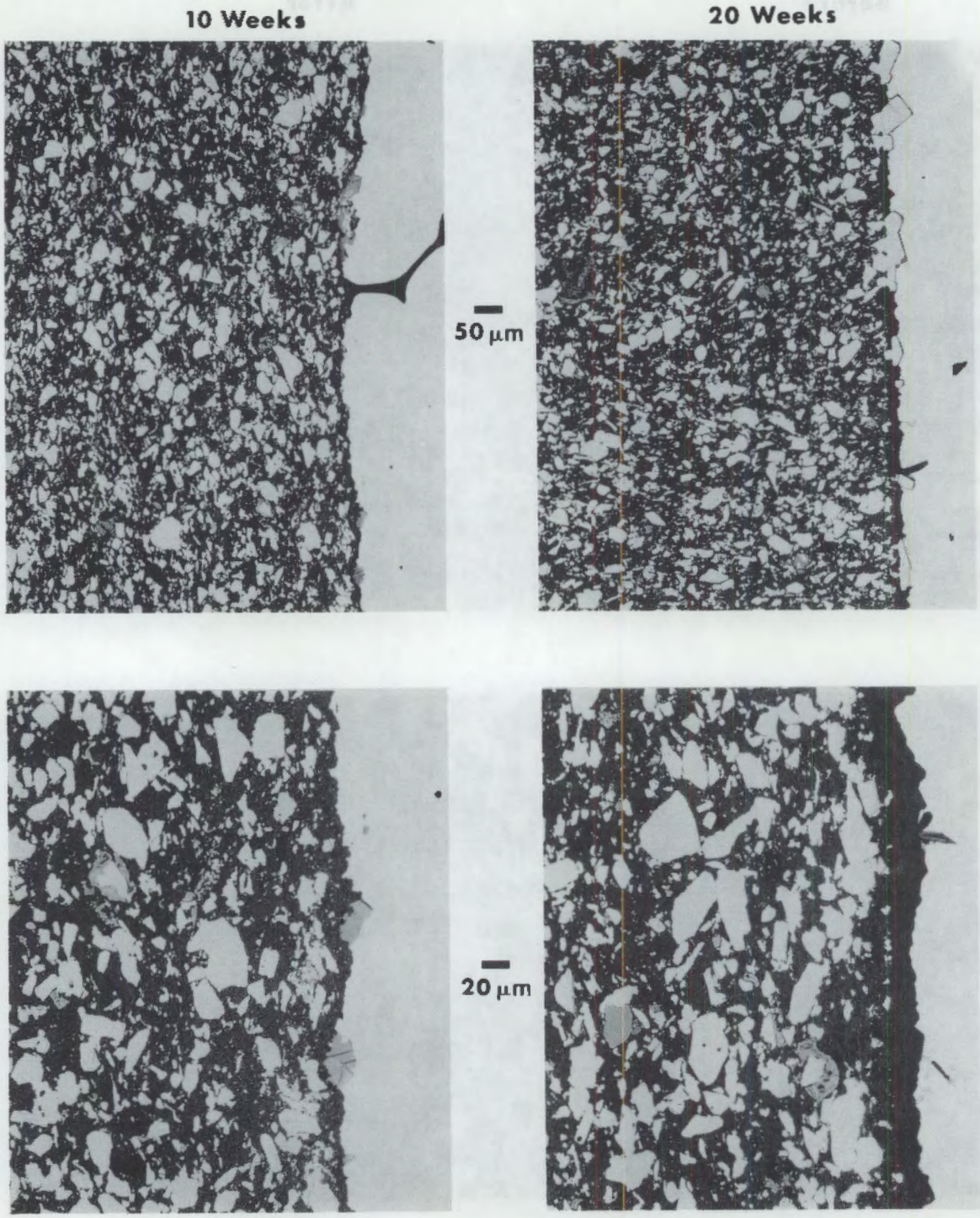

FIGURE 16. Typical Surfaces of 50 vol% TiB_2-50 vol% AlN After Exposure to Molten Al for 10 wk and 20 wk

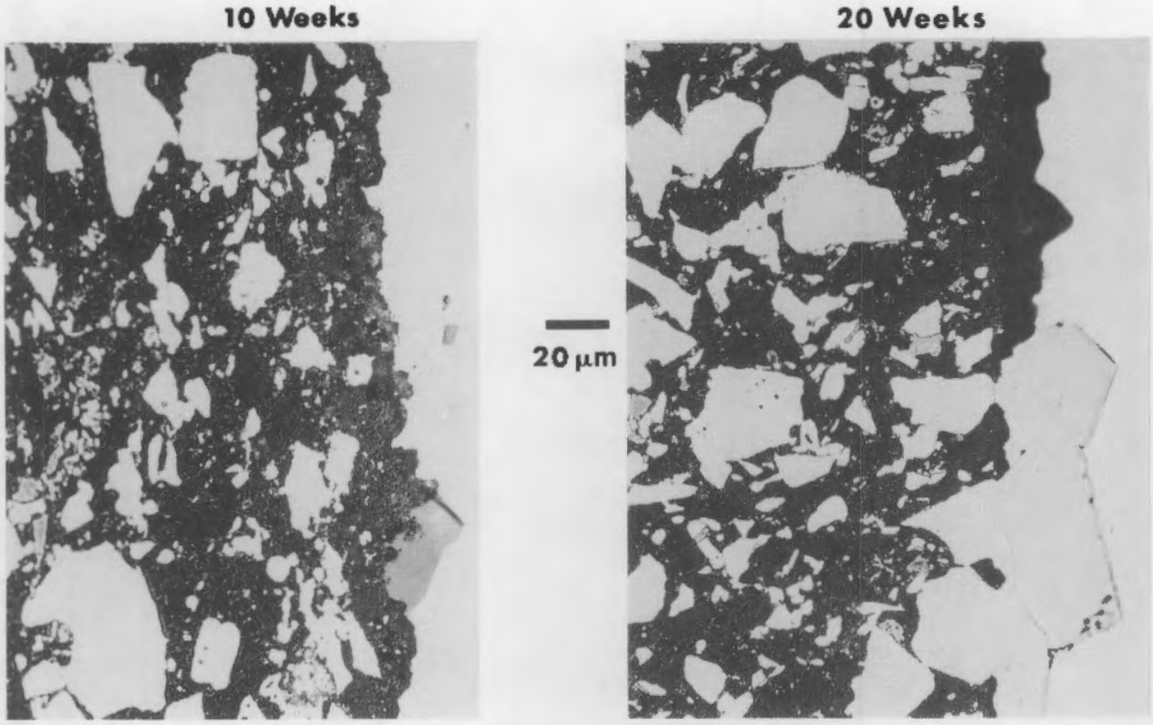

FIGURE 17. Reaction Layers at Surfaces of 50 vol% TiB_2-50 vol% AlN After Exposure to Molten Al for 10 wk and 20 wk.[2] Micrographs are taken from the same regions shown in Figure 16.

ACKNOWLEOGMENTS

Technical support by S. C. Marschman, P. E. Hart, D. M. Strachan, C. F. Windisch, N. T. Saenz, D. E. Smith, N. C. Davis, H. E. Kjarmo, H. E. Kissinger, W. Haupin, R. Keller, N. Jarrett, N. Richards and L. Joo is gratefully appreciated. The authors wish to thank M. H. Johnson and H. F. Hillegass of the Alcoa Wenatchee plant for providing spark emission spectroscopy analysis. The authors also wish to thank T. L. Gilbride and G. A. Downard for preparation of the manuscript.

REFERENCES

Andersson, C. H., and R. Warren. 1984. "Silicon Carbide Fibers and Their Potential for Use in Composite Materials." Composites. 15:16-24.

Baumgartner, H. R. 1984a. "Mechanical Properties of Densely Sintered High-Purity Titanium Diborides in Molten Aluminum Environments." J. Amer. Ceram. Soc. 67:490-497.

Baumgartner, H. R. 1984b. "Subcritical Crack Velocities in Titanium Diboride Under Simulated Hall-Heroult Cell Conditions," Amer. Ceram. Soc. Bull. 63:1172.

Baumgartner, H. R., and R. A. Steiger. 1984. "Sintering and Properties of Titanium Diboride Made From Powder Synthesized in a Plasma-Arc Heater," J. Amer. Ceram. Soc. 67(3):207-212.

Billiehaug, K. and H. A. Oye. 1980. "Inert Cathodes for Aluminum Electrolysis in Hall-Heroult Cells (I)," Aluminium 56:642.

Brandes, E. A. 1983. Smithells Metals Reference Book, 6th ed. Butterworth and Co., Ltd. London, p. 14-7.

Brondyke, K. J. 1953. "Effect of Molten Aluminum on Alumina - Silica Refractories," J. Amer. Ceram. Soc. 36(5):171-174.

Caputo, A. J., and W. J. Lackey. 1984. "Fabrication of Fiber-Reinforced Ceramic Composites by Chemical Vapor Infiltration," In Ceramic Engineering and Science Proceedings, 5(7-8):654-667, American Ceramic Society, Columbus, Ohio.

Caputo, A. J., W. J. Lackey, and D. P. Stinton. 1985. "Development of a New, Faster Process for the Fabrication of Ceramic Fiber Reinforced Ceramic Composites by Chemical Vapor Infiltration." In Ceram. Eng. Sci. Proc. 6(7-8):694-706. American Ceramic Society, Columbus, Ohio.

Chaim, R., A. H. Heuer, and R. T. Chen. 1988. "Microstructural and Microchemical Characterization of SiC-Based Fibers Produced from Polymer Precursors," Advanced Ceramic Materials, American Ceramic Society, Westerville, Ohio.

Clark, T. J., R. M. Arons, J. B. Stamatoff, and J. Rabe. 1985. "Thermal Degradation of Nicalon SiC Fibers," In Ceramic Engineering and Science Proceedings. 6(7-8):576-88, American Ceramic Society, Columbus, Ohio.

Dorward, R. C. 1973a. "Aluminum Carbide Formation and Removal During Electrolytic Reduction and Hot Metal Processing Operations," Light Metals 1973, American Institute of Mining and Metallurgical Engineers, New York. pp. 105-118.

Dorward, R. C. 1973b. "Aluminum Carbide Contamination of Molten Aluminum," Aluminium 49:686-688.

Grjotheim, K., R. Naeumann, and H. A. Oye. 1977. "Formation of Aluminum Carbide in the Presence of Cryolite Melts," Light Metals 1977, American Institute of Mining and Metallurgical Engineers, New York, pp. 233-242.

Hart, P. E., B. B. Brenden, N. C. Davis, O. H. Koski, S. C. Marschman, K. H. Pool, C. H. Schilling, C. F. Windisch, and B. J. Wrona. 1987. Inert Anode/Cathode Program Fiscal Year 1986 Annual Report. PNL-6247, Pacific Northwest Laboratory, Richland, Washington, pp. 3.18-3.21.

Hoejke, H. H. 1981. "Submicron Titanium Boride Powder and Method for Preparing Same," U.S. Patent 4,282,195.

Hollingshead, E. A., and J. A. Brown. 1981. "Rate of Solution of Carbon in Molten Aluminum Under a Cryolite Melt," Light Metals 1981, American Institute of Mining and Metallurgical Engineers, New York, pp. 625-634.

Johnson, S. M., R. D. Brittain, R. H. Lamoreaux, and D. J. Rowcliffe. 1988. "Degradation Mechanisms of Silicon Carbide Fibers," J. American Ceramic Soc., 71(3):C.132-C.135.

Jones, R. H., C. H. Henager, Jr., C. H. Schilling, L. H. Schoenlein, W. J. Weber, and F. Gac. 1988. "Interfacial Chemistry - Structure and Fracture of Ceramic Composites." In Proceedings of the American Ceramic Society: 12th Annual Conference on Composites and Advanced Ceramics. Cocoa Beach, Florida.

Kubaschewski, O., and C. B. Alcock. 1979. Metallurgical Thermochemistry. 5th Edition, p. 378, Pergamon Press, New York.

Luthra, K. L. 1986. "Thermochemical Analysis of the Stability of Continuous 'SiC' Fibers." J. Amer. Ceram. Soc. 69:C231-C233.

Mah, T., N. L. Hecht, D. E. McCullum, J. R. Hoenigman, H. M. Kim, A. P. Katz, and H. A. Lipsitt. 1984. "Thermal Stability of SiC Fibers (Nicalon)." J. Mater. Sci. 19:1191-1201.

Romine, J. C. 1987. "New High-Temperature Ceramic Fiber." In Ceram. Eng. Sci. Proc., 8(7-8):755-765, American Ceramic Society, Columbus, Ohio.

Schilling, C. H., D. I. Hagen, and P. E. Hart. 1987. Stable Attachment of TiB_2-Based Cathodes for the Aluminum Industry: Review and Recommendation, PNL-6144. Pacific Northwest Laboratory, Richland, Washington.

Schilling, C. H. 1988. Laboratory Testing of TiB_2-Based Cathodes for Electrolytic Production of Aluminum, PNL-6594, Pacific Northwest Laboratory, Richland, Washington.

Schoenlein, L. H., R. H. Jones, C. H. Henager, Jr., C. H. Schilling, and F. Gac. 1988. "Interfacial Chemistry - Structure and Fracture of Ceramic Composites." In Proc. 1988 Spring Meeting of the Materials Research Society, April 4, Reno, Nevada, Materials Research Society, Pittsburgh, Pennsylvania.

Simon, G., and A. R. Bunsell. 1984. "Creep Behavior and Structural Characterization at High Temperatures of Nicalon SiC Fibers." J. Mater. Sci. 19:3658-3670.

Standage, A. E., and M. S. Gani. 1967. "Reaction Between Vitreous Silica and Molten Aluminum," J. Amer. Ceram. Soc. 50(2):101-105.

Stinton, D. P., A. J. Caputo, R. A. Lowden, and T. M. Besmann. 1986. "Improved Fiber-Reinforced SiC Composites Fabricated by Chemical Vapor Infiltration," Ceramic Engineering and Science Proceedings, July-August 1986, American Ceramic Society, Columbus, Ohio, pp. 983-989.

Tabereaux, A. T. 1987. "Stable TiB_2-Graphite Cathodes for Aluminum Production." In Cathode Workshop Proceedings, Light Metals Production Research Group, February 27-28, Carnegie-Mellon University.

Takemoto, M., T. Yashimoto, K. Oida, and L. Yanagida. 1963. "Effect of Holding on Some Properties of Metal Tapped from Electrolytic Cells," in Extractive Metallurgy of Aluminum, Volume 2, Aluminum, G. Gerard, editor, Interscience, New York, pp. 435-452.

Tucker, K. W., J. R. Shaner, J. T. Gee, and L. A. Joo. 1986. "TiB_2-Graphite Cathodes in Aluminum Reduction Cells." In Extended Abstracts; Electrochemical Society Fall Meeting, San Diego, California.

Weast, R. C., Astle, M. J., and Beyer, W. H. 1985. CRC Handbook of Chemistry and Physics Sixty-Sixth Edition. CRC Press, Boca Raton, Florida, p. B-68 and p. B-84.

APPENDIX

ALUMINUM CARBIDE (Al_4C_3) MOLAR VOLUME ANALYSIS DURING NONPOLARIZED EXPOSURE OF TITANIUM DIBORIDE-GRAPHITE TO ALUMINUM AT 970°C

APPENDIX

ALUMINUM CARBIDE (Al_4C_3) MOLAR VOLUME ANALYSIS DURING NONPOLARIZED EXPOSURE OF TITANIUM DIBORIDE-GRAPHITE TO ALUMINUM AT 970°C

Sample calculations are presented to estimate the volumetric amount of Al_4C_3 formed by direct reaction between graphite and elemental Al, and the minimum amount of Al required to uniformly dissolve Al_4C_3 that forms by all of the graphite originally available in a TiB_2-G immersion test sample. The following properties are assumed:

- The Al_4C_3 mass density = 2.36 g/cm^3 and molecular weight = 143.96 g/mol[(a)]
- The Al liquid mass density = 2.385 g/cm^3 and molecular weight = 26.98 g/mol[(b)]
- The graphite mass density = 2.25 g/cm^3 and molecular weight = 12.0 g/mol[(a)]
- Apparent volume of each TiB_2-G sample = 1 cm^3
- Amount of Al originally present = 50 g (approximately 21 cm^3)
- Saturation solubility of 0.04 wt% Al_4C_3 in Al (Dorward 1973a and 1973b)
- Amount of graphite originally present = 17% by volume (Tabereaux 1987).

$$\frac{\text{cm}^3\ Al_4C_3}{2.36\ \text{g}\ Al_4C_3} \times \frac{143.96\ \text{g}\ Al_4C_3}{\text{mole}\ Al_4C_3} \times \frac{\text{mole}\ Al_4C_3}{3\ \text{mole C}} \times \frac{2.25\ \text{g C}}{\text{cm}^3\ \text{graphite}} \times \frac{\text{mole C}}{12\ \text{g C}}$$

$$= \frac{3.813\ \text{cm}^3\ Al_4C_3}{\text{cm}^3\ \text{graphite}}$$

(a) Weast, Astle, and Beyer 1985.
(b) Brandes 1983.

$$\frac{0.17\ cm^3 graphite}{cm^3 TiB_2\text{-}G} \times \frac{3.813\ cm^3\ Al_4C_3}{cm^3\ graphite} \times \frac{2.36\ g\ Al_4C_3}{cm^3\ Al_4C_3} \times \frac{99.06\ g\ Al}{0.04\ g\ Al_4C_3} \times \frac{cm^3\ Al}{2.385\ g\ Al}$$

$$= \frac{1588.5\ cm^3\ Al}{cm^3\ TiB_2\text{-}G}$$

The former equation suggests that 3.8 cm^3 of Al_4C_3 are formed by each cubic centimeter of graphite consumed in the $4Al + 3C \rightarrow Al_4C_3$ reaction.

The latter equation suggests that a minimum of approximately 75.6 times the original mass of Al is needed in each test crucible to uniformly dissolve Al_4C_3 formed by all of the C originally available. Therefore, it may be suggested that Al_4C_3 saturation was reached within the Al-filled TiB_2 pores near graphite-Al interfaces during the immersion tests. As a result, dissolution rates would approach zero in these regions, and Al_4C_3 crystals would be expected to accumulate and remain inside the TiB_2 pores.

DISTRIBUTION

No. of Copies

OFFSITE

M. J. McMonigle
U.S. Department of Energy
Office of Industrial Programs
Forrestal Building
Washington, DC 20585

T. J. Gross
U.S. Department of Energy
Office of Industrial Programs
Forrestal Building
Washington, DC 20585

R. L. Sheneman
U.S. Department of Energy
Office of Industrial Program
Forrestal Building
Washington, DC 20585

10 DOE Office of Scientific and Technical Information

M. Adkins
National Southwire Aluminum Company
P.O. Box 500
Hawesville, KY 42348

J. V. Anderson
WCVE3
EG&G Idaho, Inc.
Idaho Falls, ID 83415

D. Auburg
Bonneville Power Administration
P.O. Box 3621, PDX 97208
Portland, OR 97208

F. W. Baker
Ceramics Division
Alcoa Laboratories
Alcoa Center, PA 15069

No. of Copies

M. Baltzell
Eastalco Aluminum Company
Alumax, Inc.
5601 Manor Woods
Frederick, MD 21701

J. A. Barclay
U.S. Bureau of Mines
2401 "E" Street N.W.
Washington, DC 20241

W. L. Barham
Kaiser Aluminum and Chemical Corp.
P.O. Box 877
Pleasanton, CA 94566

H. Robert Baumgartner
Ceramics Division
Alcoa Laboratories
Alcoa Center, PA 15069

T. R. Beck
Electrochemical Technology Corp.
1601 Dexter Avenue
Seattle, WA 98109

S. Berwagan
Bonneville Power Administration
P.O. Box 3621 K
Portland, OR 97208

T. M. Besmann
Metals and Ceramics Division
Oak Ridge National Laboratory
P.O. Box X, Bldg. 4515
Oak Ridge, TN 37831-6063

K. A. Blakely
President
Advanced Refractory Technologies, Inc.
699 Hertel Ave.
Buffalo, NY 14207

No. of
Copies

M. H. Blenk
Du Pont
P.O. Box 787
Niagara Falls, NY 14302

L. G. Boxall
Martin Marietta Laboratories
1450 South Rolling
Baltimore, MD 21227

J. Bracher
Kaiser Aluminum and Chemical
Corp.
825 N.E. Multnomah St.,
Suite 960
Portland, OR 97232-2150

R. Bradt
Department of Materials Science
and Engineering
University of Washington FB-10
Seattle, WA 98195

J. J. Brown, Jr.
Materials Engineering
Virginia Polytechnic Institute
Blacksburg, VA 24061

A. Budner
Bonneville Power Administration
P.O. Box 3621--EPC
Portland, OR 97208

A. J. Caputo
Metals and Ceramics Division
Oak Ridge National Laboratory
P.O. Box X
Oak Ridge, TN 37831-6063

N. Clark
Bonneville Power Administration-
Industrial Conservation
P.O. Box 3621
Portland, OR 97208

No. of
Copies

A. Cooke
Martin Marietta Laboratories
1450 South Rolling
Baltimore, MD 21227

J. A. Coppola
Standard Oil Engineered
Materials Company
P.O. Box 156
Niagara Falls, NY 14302

R. Curtis
Materials Development
Corporation
81 Hicks Avenue
Medford, MA 02155

J. V. Day
Mail Drop 2232
Kaiser Aluminum and Chemical
Corp.
300 Lakeside Drive
Oakland, CA 94643

R. Dethlefsen
Maxwell Laboratories
8888 Balboa Ave.
San Diego, CA 92123

D. H. DeYoung
Alcoa Technical Center
Alcoa Center, PA 15069

S. Diamond
Battelle Columbus Laboratories
505 King Avenue
Columbus, OH 43201-2693

C. W. Doerr
The Stackpole Corporation
Cermag Division
201 Stackpole Street
St. Marys, PA 15857

No. of
Copies

R. C. Dorward
Kaiser Aluminum and Chemical
Corp.
P.O. Box 877
Pleasanton, CA 94566

G. L. Eitel
Stone & Webster Engineering
Corp.
Greenwood Plaza Box 5406
Denver, CO 80217

R. Engdahl
Deposits and Composites, Inc.
318 Victory Drive
Herndon, VA 22070

J. F. Elliott
MIT
Room 4-138
77 Massachusetts Avenue
Cambridge, MA 02139

B. G. Epstein
A. D. Little, Inc.
600 Maryland Ave., S.W.
Washington, DC 20024

J. W. Evans
University of California
Dept. of Matl. Sci. and Mineral
Eng.
Berkeley, CA 94720

R. A. Fenimore
ICI Advanced Materials
Rollins Building, Eighth Floor
Wilmington, DE 19897

D. A. Figgins
ARCO Petroleum Products Co.
P.O. Box 61004
Anaheim, CA 92803-6104

T. Foley
Northwest Power Planning Council
850 S.W. Broadway, Suite 1100
Portland, OR 97205

No. of
Copies

P. Foster
Alcoa Laboratories
P.O. Box 772
New Kensington, PA 15068

J. Gee
Great Lakes Research Corp.
P.O. Box 1031
Elizabethton, TN 37643

T. Gilligan
Eltech Systems Corp.
625 East Street
Fairport Harbor, OH 44077

W. M. Goldberger
Superior Graphite Co.
120 S. Riverside Plaza
Chicago, IL 60606

J. Goodwell
Center for Metals Production
Mellon Institute
4400 Fifth Avenue
Pittsburgh, PA 15213

J.A.S. Green
Martin Marietta Laboratories
1450 South Rolling
Baltimore, MD 21227

C. Griffin
Ceramatec Inc.
2425 S. 900 West
Salt Lake City, UT 84119

L. I. Grindstaff
Great Lakes Research Corp.
P.O. Box 1031
Elizabethon, TN 37643

J. Haggerty
MIT
Building 12, Room 009
77 Massachusetts Avenue
Cambridge, MA 02139

No. of
Copies

I. L. Harry
Electric Power Research
Institute
P.O. Box 10412
Palo Alto, CA 94303

W. Haupin
2820 7th Street Road
Lower Burrell, PA 15068

H. W. Hayden, Jr.
1419 East 21st Street
The Dalles, OR 97058

R. Hill
Union Carbide Corp.
P.O. Box 94637
Cleveland, OH 44101

H. F. Hillegass
Alcoa Wenatchee Works
P.O. Box 221
Wenatchee, WA 98807

D. G. Howitt
College of Engineering
University of California, Davis
Davis, CA 95616

G. R. Hyde
U.S. Bureau of Mines
2401 "E" Street N.W.
Washington, DC 20241

S. C. Jacobs
Primary Processing
Aluminum Company of America
Alcoa Technical Center
Alcoa Center, PA 15069

R. A. James
Kaiser Aluminum and Chemical
Corp.
E2111 Hawthorne Road
Mead, WA 99021

No. of
Copies

S. H. Jan
Tennessee Valley Authority
1850 Commerce Union Bank Bldg.
Chattanooga, TN 37401

N. Jarrett
149 Jefferson Avenue
New Kensington, PA 15068

J. Joesowicz
Material Development Laboratory
Atlantic Richfield
20717 Prairie Street
Chatsworth, CA 91311

A. R. Johnson
Kaiser Aluminum
P.O. Box 877
Pleasanton, CA 94366

J. Johnson
Intalco Aluminum Company
P.O. Box 937
Ferndale, WA 98248

M. H. Johnson
Alcoa Wenatchee Works
P.O. Box 221
Wenatchee, WA 98801

L. Joo
Great Lakes Research Corp.
P.O. Box 1031
Elizabethon, TN 37643

M. Karmous
Oregon State Department of
Energy
625 Marion Street, N.E.
Salem, OR 97310

R. Keller
RD 3
Roundtop Road
Export, PA 15632

No. of
Copies

C. Anderson
Columbia Aluminum Co.
85 John Day Dam Road
Goldendale, WA 98620

K. Krupinski
Mail Stop 57
U.S. Steel Technical Center
1 Technical Center Drive
Monroeville, PA 15146

G. Y. Lai
Cabot Corporation
P.O. Box 9013
Kokomo, IN 46902-9013

J. E. Lane
Ceramic Research and
Development Center
Westinghouse Electric
Corporation
1310 Beulah Road
Pittsburgh, PA 15235

Sai-Kwing Lau
Standard Oil Engineered
Materials Company
Niagara Falls R&D Center
P.O. Box 832
Niagara Falls, NY 14302

J. J. Leddy
Dow Chemical U.S.A.
1776 Building
Midland, MI 48640

W. W. Liang
Gas Research Institute
8600 West Bryn Mawr Avenue
Chicago, IL 60631

W. G. Lindman
P.O. Box 567
Boyerstown, PA 19512

No. of
Copies

W. H. Link
Columbia Aluminum Corp.
85 John Day Dam Road
Goldendale, WA 98620

Steve Loftness
Washington State Energy Office
400 E. Union
Olympia, WA 98504

W. Long
Building B815
Dow Chemical
Freeport, Texas 77541

R. A. Lowden
Metals and Ceramics Division
Oak Ridge National Laboratory
P.O. Box X, Bldg. 4515
Oak Ridge, TN 37831-6063

W. N. Maclay
Koppers Company, Inc.
440 College Park Drive
Monroeville, PA 15146

V. H. Markant
Du Pont
P.O. Box 787
Niagara Falls, NY 14302

C. J. McMinn
Extractive Metallurgical
Department
Reynolds Metals Company
P.O. Box 1200
Sheffield, AL 35660

C. H. McMurtry
Standard Oil Engineered
Materials Company
Niagara Falls R&D Center
P.O. Box 832
Niagara Falls, NY 14302

No. of
Copies

M. A. Mittnick
Avco Specialty Materials
Subsidiary of Textron Inc.
2 Industrial Avenue
Lowell, MA 01851

A. Moussa
A. D. Little, Inc.
20 Acorn Park
Cambridge, MA 02140

B. C. Mutsuddy
Battelle Columbus Division
505 King Avenue
Columbus, OH 43201-2693

A. N. Patel
Battelle Columbus Laboratories
505 King Avenue
Columbus, OH 43201-2693

J. R. Payne
Kaiser Aluminum and Chemical
Corp.
P.O. Box 877
Pleasanton, CA 94566

W. Pebley
Oregon Freeze Dry Corp.
525 25th Ave SW
P.O. Box 1048
Albany, OR 97321

K. Peterson
Columbia Aluminum Corp.
85 John Day Dam Road
Goldendale, WA 98620

R. D. Peterson
Reynolds Metals Company
P.O. Box 1200
Sheffield, AL 35660

T. R. Prichett
Kaiser Aluminum and Chemical
Corp.
P.O. Box 877
Pleasanton, CA 94566

No. of
Copies

W. W. Pritsky
Aluminum Association
900 19th St. N.W.
Washington, DC 20006

S. P. Ray
Alcoa Technical Center
Alcoa Center, PA 15069

J. F. Rhodes
Advanced Composite Materials
Corp.
1525 S. Buncombe Rd.
Greer, SC 29651

N. E. Richards
Reduction Laboratory
Reynolds Aluminum Corporation
P.O. Box 1200
Sheffield, AL 35660

J. J. Ritter
Ceramics Division
National Bureau of Standards
Gaithersburg, MD 20899

R. C. Rohwedder
3028 Ohio Street
Longview, WA

J. Rosling
Myers Metals and Minerals
459 Colman Building
Seattle, WA 98104

D. R. Sadoway
MIT
Room 8-109
77 Massachusetts Avenue
Cambridge, MA 02139

W. Scott
Department of Materials Science
& Engineering
Wilcox Hall FB-10
University of Washington
Seattle, WA 98195

No. of
Copies

D. R. Secrist
Great Lakes Research Corp.
P.O. Box 1031
Elizabethon, TN 37643

A. B. Shah
Noranda Aluminum, Inc.
P.O. 8ox 70
New Madras, MO 63869

N. Shelton
Intalco
1300 S.W. 5th, Suite 3508
Portland, OR 97201

F. W. Spillers
Dow Chemical U.S.A.
B-1210 Building
Freeport, TX 77541

D. V. Stewart
Reynolds Metals Co.
P.O. Box 1200
Sheffield, AL 35660

D. Strahan
Reynolds Metals Company
P.O. Box 27003
Richmond, VA 23261

A. T. Tabereaux
Reynolds Metals Company
P. O. Box 1200
Sheffield, AL 35660

G. P. Tarcy
Aluminum Company of America
Alcoa Technical Center
Alcoa Center, PA 15069

P. Thaure
Primary Planning and Production
Alumax
400 S. El Camino Rd.
San Mateo, CA 94402

No. of
Copies

W. H. Thielbahr
Conservative Technology
Division
DOE-Idaho Operations Office
785 DOE Place
Idaho Falls, ID 83402

R. Unger
Merner Research
P.O. Box 248
Ridgewood, NJ 07451

A. Vinnard
Bonneville Power Administration
(KWI)
P.O. Box 3621
Portland, OR 97208

T. Von Muller-KWI
Bonneville Power Administration
P.O. Box 3621
Portland, OR 97208

D. H. Weinblatt
AIMCOR
One Parkway North
Deerfield, IL 60015

J. D. Weyand
Alcoa Technical Center
Alcoa Center, PA 15069

B. Wilcox
Northwest Aluminum Co.
3313 W. Second St.
The Dalles, OR 97058

C. B. Wilson
Dow Chemical U.S.A.
Texas Operations
B-101 Building
Freeport, TX 77541

W. Winnard
Battelle Washington Office
2030 "M" Street N.W.
Washington, DC 20036

No. of
Copies

J. C. Withers
Keramont Research Corporation
4233 S. Fremont Avenue
Tucson, AZ 85714

W. A. Zdaniewski
Engelhard Corporation
Menlo Park, CN28
Edison, NJ 08818

FOREIGN

D. Brodie
Comalco Ltd.
55 Collins St.
Melbourne, AUSTRALIA

T. Kjar
Comalco Ltd.
55 Collins St.
Melbourne, AUSTRALIA

E. W. Dewing
Alcan International
P.O. Box 8400
Kingston, Ontario
CANADA K7L 4Z4

T. J. Hudson
Alcan International
2001 rue University
C.P. 6090
Montreal, Quebec
CANADA H3C 3H2

D. N. MacMillan
Alcan International
C.P. 1250
Jonquieve, Quebec
CANADA G7S 4K8

No. of
Copies

T. Rawlings
Alcan International Limited
Engineering Division
C.P. 6090
Montreal, Quebec
CANADA, H3C 3H2

J. H. Reimers
Jan H. Reimers and Associates
Inc.
221 Lakeshore Road East
Oakville, Ontario
CANADA L6J 1H7

A. Oye
Institute of Inorganic
Chemistry
Norwegian Institute of
Technology
University of Trondheim
N-7034 Trondheim-NTH, NORWAY

J. Thonstad
Laboratories of Industrial
Electrochemistry
Norwegian Institute of
Technology
University of Trondheim
N-7034 Trondheim-NTH, NORWAY

K. O. Vee
ASV
Ardal Verk
N-5875 Ardalstargen, NORWAY

ONSITE

DOE Richland Operations Office

E. C. Norman

No. of
Copies

60 Pacific Northwest Laboratory

K. E. Bailey
M. Clement
N. C. Davis
G. J. Exarhos
J. R. Divine
T. L. Gilbride
G. L. Graff (10)
P. E. Hart
R. H. Jones
S. C. Marschman
G. L. McVay
N. L. Moore
C. H. Schilling (30)
M. Danielson
D. M. Strachan
Publishing Coordination (2)
Technical Report Files (5)